

Numerical methods for inertial confinement fusion

X. Blanc¹, B. Després²

¹ CEA, DAM, DIF,
Bruyères-le-Chatel, F-91297 Arpajon, France.

² Université Pierre et Marie Curie-Paris6,
UMR 7598, laboratoire Jacques-Louis Lions,
4 place Jussieu, F-75252 Paris Cedex 05, France.

July 17, 2010

Contents

1	Introduction	5
1.1	Physical setting	5
1.2	Modelling	8
1.3	Numerical methods	11
2	Hydrodynamics	13
2.1	Lagrangian viewpoint	13
2.2	The Euler-Lagrange change of variable in conservation laws	14
2.2.1	Dimension one	15
2.2.2	Dimension two	15
2.2.3	Entropy	16
2.2.4	Hyperbolicity	16
2.3	Schemes in dimension one	17
2.4	Schemes in dimension 2 or 3	18
2.4.1	A nodal solver	19
2.4.2	A generic Lagrangian scheme in arbitrary dimension	19
2.5	Some numerical results	20
2.5.1	The Kidder problem	20
2.5.2	A perturbation problem	22
2.6	Numerical analysis	22
2.7	Multi-temperature models	23
3	Radiative transfer	27
3.1	Radiative transfer equation	27
3.1.1	Free streaming limit	28
3.1.2	Diffusion limit	28
3.1.3	Boundary conditions in the diffusion limit	29
3.2	Mathematical analysis	30
3.2.1	Existence results for the radiative transfer equation	30
3.2.2	Rigorous justification of the diffusion limit	31
3.2.3	Marshak waves	34
3.2.4	Flux limitation	35
3.3	Numerical schemes	36
3.3.1	Multigroup approximation	36
3.3.2	Time and space discretization	37
3.4	Higher order models	43
4	Hele-Shaw models	47
4.1	Introduction	47
4.2	The quasi-isobar model	49
4.3	Hele-Shaw models	50

Chapter 1

Introduction

Nuclear fusion reactions is the source of energy of stars, and is the major source of energy in the visible universe. In stellar objects, gravitational forces confine the fusion fuel, which reaches conditions for nuclear fusion reactions. This route can of course not be followed for energy production on earth. Therefore, mainly two alternate ways are proposed to date: magnetic confinement, for instance in ITER (International Thermonuclear Experimental Reactor) project, or inertial laser confinement, for instance in NIF (National Ignition Facility) or LMJ (Laser MégaJoule) project. In both cases, the reaction under study is the combination of deuterium and tritium atoms:



which produces an energy of 17.6 MeV, that is, 410 kJ per gram. Reaction (1.1) is the most favorable (in terms of production of energy) fusion reaction of hydrogen isotopes. In inertial confinement fusion, the fuel is heated by laser pulses, hopefully reaching condition under which a significant mass of hydrogen undergoes reaction (1.1). The NIF project, in Livermore, California, started in 1997, and delivered its first experiment in 2009. It uses 192 high power laser beams. These lasers are amplified from a single source, along a 300 meters long travel. Then, they are driven to an experiment chamber, which is a sphere of 10 meters diameter, and concentrated onto a fuel target, which size is a few millimeters. The LMJ, in Bordeaux, France, is based on the same concept, with 160 beams. It is expected to be operating in 2014.

1.1 Physical setting

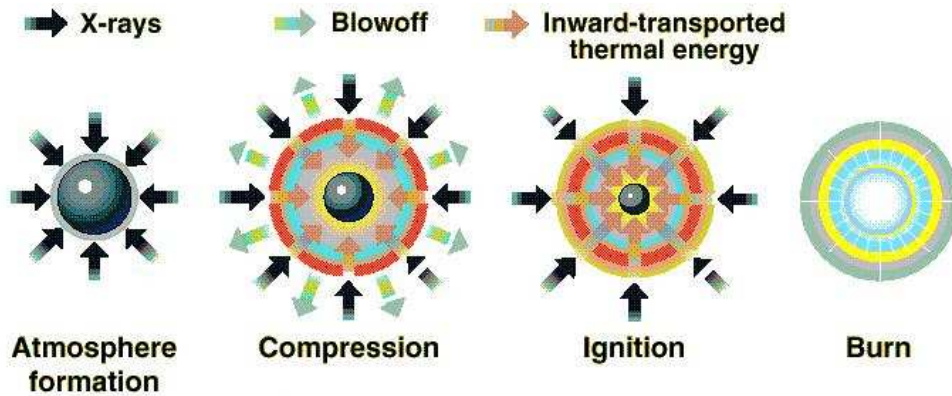
The principle used in a laser facility such as NIF or LMJ is to design a small plastic ball filled with hydrogen, which is heated by laser beams or soft X-rays. The outer layer is heated first, and therefore is dilated. The momentum conservation then implies that inner layers of gas are contracted. Thus, the core of the ball implodes and heats up. This creates a "hot spot" at the center of the capsule (see figure 1.4). The fusion reaction then start at the center, and burn out all the fuel of the capsule (see figure 1.1). Lawson gave in [84] a criterion for reaching nuclear fusion reactions in a confined plasma. This criterion may be used to indicate the conditions to reach at the hotspot. It links the density ρ with the temperature T and the confinement time τ . This criterion reads

$$\rho T \tau \gtrsim 10^{-5} \text{ K} \cdot \text{s} \cdot \text{g} \cdot \text{cm}^{-3}.$$

The validity domain of this criterion is $10^7\text{K} \leq T \leq 5 \times 10^8\text{K}$. The confinement time cannot be greater than the time for a rarefaction wave to travel through the plasma, $\tau \approx R/c_s$, where R is the radius of the plasma, and c_s the sound speed. This gives the following:

$$T \approx 10^7\text{K}, \quad \tau \approx 10^{-9}\text{s}, \quad \rho R \approx 0.3\text{g} \cdot \text{cm}^{-2}.$$

Such values can be reached at the hot spot during the above-mentionned process of heating a small ball of fuel. This can be done by direct drive, or by indirect drive.



The X-rays rapidly (1) heat the capsule, (2) causing its surface to fly outward. This outward force causes an opposing inward force that compresses the fuel inside the capsule. When the compression reaches the center, temperatures increase to 100,000,000 °C, (3) igniting the fusion fuel and (4) producing a thermonuclear burn that yields many times the energy input (energy gain).

Figure 1.1: Scheme of the inertial confinement fusion process.

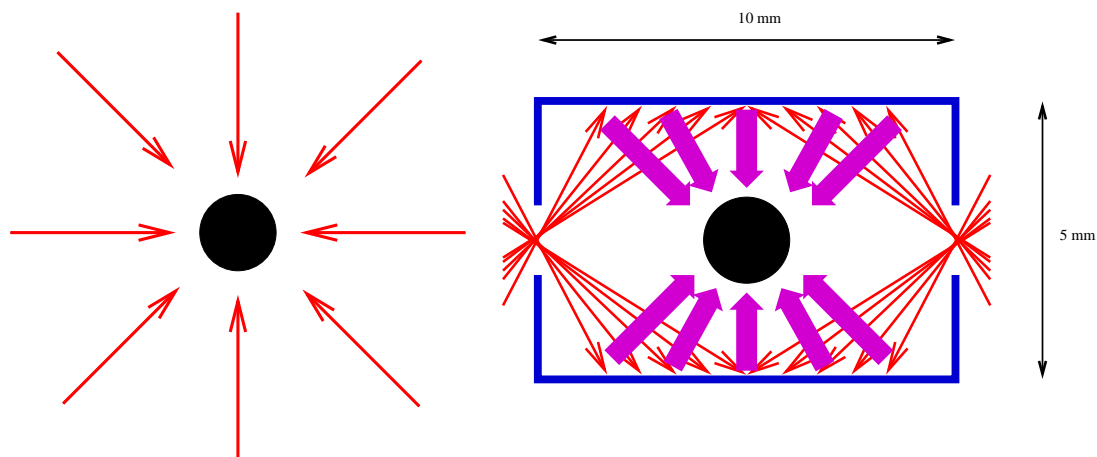


Figure 1.2: Direct drive (left) and indirect drive (right)

Direct drive. In this situation, the laser beams are pointed towards the capsule and directly heat it (see figure 1.2). The advantage here is that all the power of the lasers is used to heat the capsule. However, the heating is not uniform, therefore the implosion is not spherically symmetric. Hence, instabilities develop during the process. This may result in a considerable loss of energy. See figure 1.3.

Indirect drive. In this second approach, the capsule is inside a cavity, or hohlraum, composed of high-Z material (typically gold). The laser beams point towards the inner boundaries of the hohlraum. The lasers heat the walls of the hohlraum, which emit X-rays towards the capsule. The advantage of this approach is two-fold: first, the heating of the capsule is more uniform, which minimizes hydrodynamical instabilities. Second, X-rays are usually better absorbed by the external layers of the capsule. However, the main drawback of this approach is that in the process of heating the inner wall of the cavity, up to 90% of the energy may be lost (see Figure 1.5).

A third approach, which is proposed for instance in the FIREX (Fast Ignition Realization Experiment) project, consists in imploding a fuel capsule by direct drive, then use another laser to create a hot spot inside the capsule.

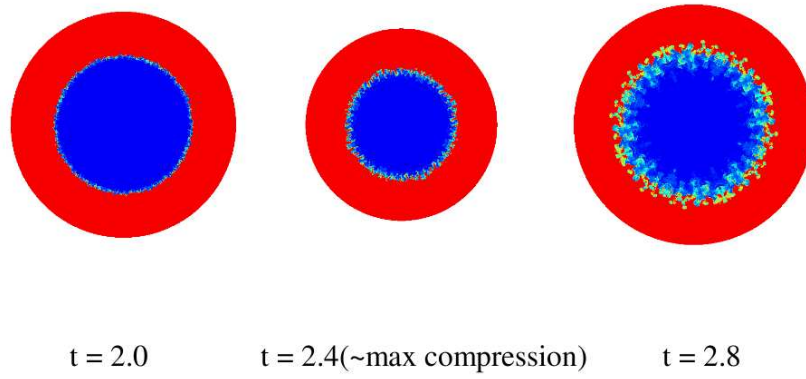


Figure 1.3: An example of development of hydrodynamical instability during the implosion of a capsule

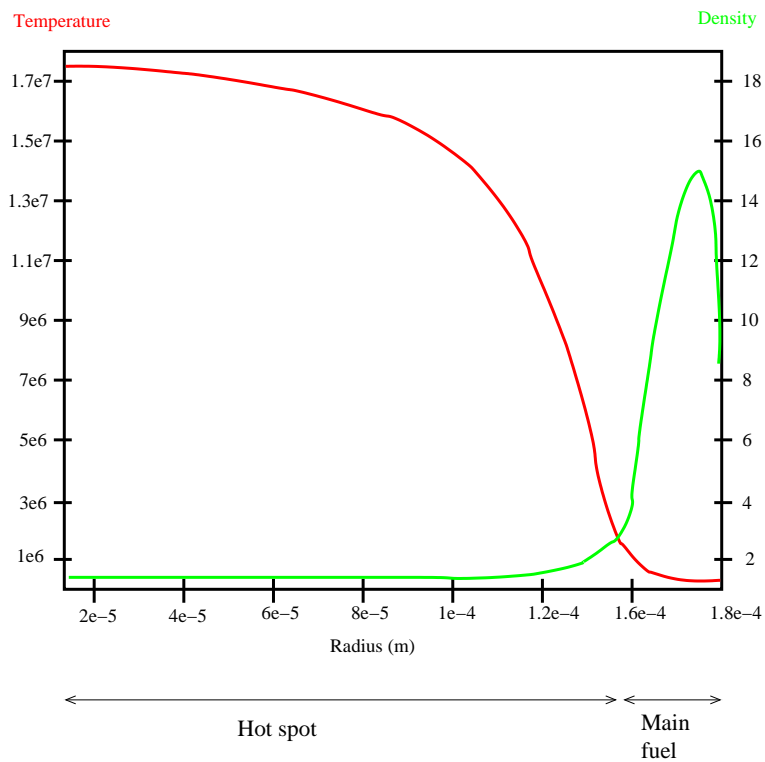


Figure 1.4: Typical hot spot configuration resulting from an implosion: density (green, in g cm^{-2}) and temperature (red, in K)

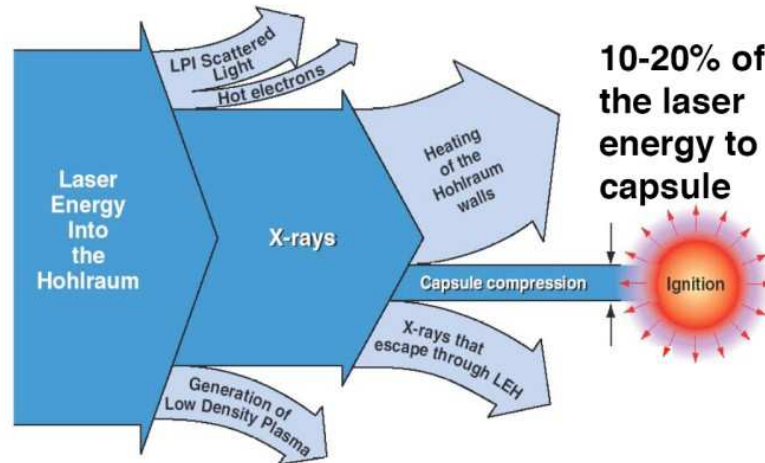


Figure 1.5: Energy loss in the indirect drive IFC process.

The strategy of indirect drive was retained both for the LMJ and NIF projects. We will therefore concentrate on this approach in the present document.

The procedure described above is of course very delicate, and the use of numerical simulation is of great importance. It helps understanding the physics and designing the different components of the target (capsule and hohlraum). To fix the ideas, an LMJ cavity is about 1 cm long and 5 mm large, while the capsule diameter is about 1 mm. At the end of the implosion, that is, when the fusion reactions are supposed to start, the heart of the target is about 50 to 100 μm large. The process lasts a few nanoseconds.

As mentioned above, the question of the development of hydrodynamical instabilities is of crucial importance, since it may have great impact on the number of reactions taking place in the fuel. Indeed, the main process at work in this kind of experiment is radiative ablation. By nature, such a process produces an ablation front which is Rayleigh-Taylor unstable. Hence, it is important for the simulations to capture the development of these instabilities.

1.2 Modelling

The modelling issues related to inertial confinement fusion are:

1. The laser plasma interaction (LPI): in the hohlraum, all materials are rapidly turned into plasmas, which present strong and complicated interactions with laser beams.
2. The hydrodynamics of the implosion: it is triggered by a succession of shocks. These result in Rayleigh-Taylor instabilities which need to be understood.
3. The coupling with radiative transfer: the plasmas emit high energy radiations which heat up the core of the capsule.

In the present document, we deliberately leave aside the question of LPI, which is not fully understood yet. We will assume that it is properly taken into account by an empirical source term in the equations of radiation hydrodynamics. For details on LPI, we refer to [129] and the references therein.

Hydrodynamics

In the following, we adopt the convention that boldface letters indicate vectors (of \mathbb{R}^2 or \mathbb{R}^3). Typically, \mathbf{x} is a position and \mathbf{u} is a velocity. The hydrodynamics of the problem is usually

assumed to be well described by compressible Euler equations for the ions and electrons:

$$\begin{cases} D_t \rho + \rho \operatorname{div}(\mathbf{u}) & = 0, \\ \rho D_t \mathbf{u} + \nabla p & = \mathbf{F}_r, \\ \rho D_t E_e + p_e \operatorname{div}(\mathbf{u}) - \operatorname{div}(\chi_e \nabla T_e) + W_{ei} & = Q_r + S, \\ \rho D_t E_i + p_i \operatorname{div}(\mathbf{u}) + \operatorname{div}(\chi_i \nabla T_i) - W_{ei} & = 0, \end{cases} \quad (1.2)$$

where $D_t = \frac{\partial}{\partial t} + \mathbf{u} \cdot \nabla$ is the derivative along the flow. The unknowns of this system are the density $\rho(\mathbf{x}, t) \in \mathbb{R}^+$ of the plasma, its velocity $\mathbf{u}(\mathbf{x}, t) \in \mathbb{R}^3$ and its pressure $p(\mathbf{x}, t) \in \mathbb{R}$. We also have electronic and ionic values: pressures $p_e(\mathbf{x}, t), p_i(\mathbf{x}, t) \in \mathbb{R}$ (with $p = p_e + p_i$), energies $E_e(\mathbf{x}, t), E_i(\mathbf{x}, t) \in \mathbb{R}$ (with $E = E_e + E_i$), and temperatures $T_e(\mathbf{x}, t), T_i(\mathbf{x}, t)$. Here, The terms \mathbf{F}_r and Q_r are the radiative sources, and S is an additional source term modelling the laser energy drop. This set of equations is closed by an adapted equation of state

$$(E_e, p_e, E_i, p_i) = \mathcal{F}(\rho, T_e, T_i). \quad (1.3)$$

This bi-temperature equation of state is not explicit, and one commonly uses tabulated versions. However, one may, for the sake of clarity, think of (1.3) as a perfect gas equation of state, in the spirit of Section 2.7 below. For the sake of simplicity, we do not take into account the contribution of fusion reactions nor supra-thermic particles, which give additional source terms in (1.2). We refer to [34] for more details.

The thermal conductivity coefficients χ_e and χ_i are usually defined by Spitzer [135] or Hubbard [69] approximations. These are highly nonlinear functions of the temperature. For instance,

$$\chi_e \propto T_e^{5/2}.$$

The coupling terms W_{ei} between electrons and ions are given by

$$W_{ei} = \rho C_{ve} \frac{m_e T_e - T_i}{m_i \tau_{ei}}, \quad (1.4)$$

where τ_{ei} is the characteristic time of relaxation between electrons and ions, and is proportional to $T_e^{3/2}$ [34, 132, 135]. Finally, \mathbf{F}_r and Q_r are the coupling terms between matter and radiation. They read

$$\mathbf{F}_r = \int_{S^2} \int_0^\infty \Omega (\sigma_a(\nu) + \kappa_{\text{Th}}) I_\nu(\mathbf{x}, t, \Omega) d\nu \frac{d\Omega}{4\pi}, \quad (1.5)$$

and

$$Q_r = \int_{S^2} \int_0^\infty (\sigma_a(\nu) I_\nu(\mathbf{x}, t, \Omega) - \sigma_e(\nu) B_\nu(T_e)) d\nu \frac{d\Omega}{4\pi}. \quad (1.6)$$

The values of the terms in the above integrands are made precise in the next paragraph.

Radiative transfer

System (1.2) is coupled with the radiative transfer equation:

$$\begin{aligned} \frac{\rho}{c} D_t \left(\frac{I_\nu}{\rho} \right) + \Omega \cdot \nabla I_\nu + \sigma_a(\nu) I_\nu - \sigma_e(\nu) B_\nu(T_e) + \frac{1}{c} (\Omega \otimes \Omega : \nabla \mathbf{u}) \left(I_\nu - \frac{\partial(\nu I_\nu)}{\partial \nu} \right) \\ + \kappa_{\text{Th}} \left(I_\nu - \int_{S^2} \frac{3}{4} \left(1 + (\Omega \cdot \Omega')^2 \right) I_\nu(\Omega') \frac{d\Omega'}{4\pi} \right) = 0, \end{aligned} \quad (1.7)$$

where $I_\nu(\mathbf{x}, t, \Omega)$ is the specific radiative intensity. It is a function of the frequency $\nu \in \mathbb{R}^+$, of the space-time variables (\mathbf{x}, t) and of the propagation direction $\Omega \in S^2$ the unit sphere of \mathbb{R}^3 . In (1.7), c is the speed of light, σ_a is the absorption cross section, σ_e is the emission cross section, and κ_{Th} is the Thomson scattering coefficient. This equation may be derived by counting up the energy carried by photons in an elementary volume of the phase space (space, time, frequency, direction) *in the comobile frame*. Note that *a priori* the change of frame is relativistic, but we have used in (1.7) the fact that \mathbf{u}/c is small to simplify the equations. We refer to the textbooks [27, 104, 112] for details (see also [22, 21]). Let us give some explanations on the different terms in this equation:

- the first two terms are simple transport terms;
- the third term models the absorption of radiation by matter;
- the fourth term models spontaneous emission of radiation by matter. The quantity $B_\nu(T_e)$ is the Planckian distribution at T_e , that is:

$$B_\nu(T_e) = \frac{2h}{c^2} \frac{\nu^3}{e^{\frac{h\nu}{kT_e}} - 1}. \quad (1.8)$$

This is the radiation emitted by a black body at temperature T_e in the vacuum [104, 112]. The fact that the emission term of (1.7) has the form (1.8) relies on the local thermal equilibrium (LTE) hypothesis (see [112, 104, 146]);

- the fifth term models the frequency shift due to the change of frame (Doppler effect);
- the last term is the Thomson scattering term, which models the collision of photons with free electrons.

Note finally that at equilibrium, that is, when $\mathbf{u} = 0$ and ρ is constant, then one should recover $I_\nu = B_\nu(T_e)$, therefore

$$\sigma_a(\nu) = \sigma_e(\nu).$$

We have neglected in the above equation several phenomenons, such as relativistic effects or angular aberration, which are believed to be negligible in the case of inertial fusion. The question of Compton scattering is less clear, and it may be included if necessary [27, 104, 112, 146].

To date, an efficient method to treat equation (1.7) in its full generality is not available. However, two limits of specific interest in themselves may be identified:

1. The *free streaming* limit, in which the matter is transparent, that is, the coefficients σ_a , σ_e and κ_{Th} are sufficiently small. In such a case, Monte Carlo methods are well adapted to solve (1.7). Such methods are described in [79] for instance.
2. The *diffusion* limit, in which the matter is opaque, that is, the quantity $\lambda(\nu) = (\sigma_a(\nu) + \kappa_{Th})^{-1}$, that is, the mean free path in (1.7), is small. In such a case, the radiative transfer equation is well approximated by a diffusion equation.

Note finally that, as mentioned above, the coupled system (1.2)-(1.7) is a model problem, which we believe exhibits the main difficulties at hand in the modelling of ICF. However, one needs to take into account additional equations (in particular neutronics and fusion reactions) in order to describe correctly the physics of the problem. For the sake of clarity, we stick to the present simplified case.

Coupling problems

In coupling the above systems (1.2) and (1.7), many problems arise.

First, it is not even known, on a theoretical level, if the system is well posed, globally in time. It is proved in [91] for the grey case (that is, when σ_a and σ_e do not depend on ν), and [147] for the general case, that local in time existence holds. See also [72] for related problems. Some results exist in the case of Navier-Stokes equation instead of Euler equation [17], in the diffusion approximation. See also [42] for related existence results in dimension one.

Second, one needs to discretize in space equations (1.2)-(1.7). Hence, the discretization of these various equations should share common features. For instance, if the temperature is assumed to be constant in a cell for (1.2), it should also be for (1.7). This induces additional constraints on the corresponding schemes.

Third, apart from the problem of space discretization, one needs to discretize in time the system (1.2)-(1.7). In this respect, a splitting strategy is often used: at each time step, (1.2) is solved first, then (1.7) is solved. The error introduced by such a splitting must be studied carefully.

1.3 Numerical methods

The numerical methods will be developed in the subsequent chapters, so we only give here the main flavor.

First, one needs to discretize (in time and space), the hydrodynamics part (1.2). This is developed in Chapter 2 below. In general, as explained in Section 2.1, Lagrangian methods are preferred for this part.

Second, the discretization of the radiative part (1.7) implies in principle discretization of space-time variables, and of frequency and propagation direction. Since this is costly, a common approach is to simplify the model by using diffusion approximation, as explained in Section 3.1.

Note that by doing so, one must face the problem of designing a diffusion scheme on a mesh which may be highly deformed. This is of course an important issue, which is (partly) studied in Section 3.3.

The last chapter of the present document gives an example of simplified model for describing the evolution of the ablation front. This model may help in understanding particular phenomena, such as, for instance, stabilization of long wavelength linear instability.

Chapter 2

Hydrodynamics

2.1 Lagrangian viewpoint

The hydrodynamic numerical simulation of compressible flows for Inertial Confinement Fusion [31, 118] makes an important use of Lagrangian methods because they are more adapted than Eulerian methods. Shortly speaking Eulerian methods are written in the laboratory frame, while Lagrangian methods are written in the fluid frame. Assets of Lagrangian methods are

- easy discretization of free boundaries (external and internal),
- naturally adapted for multimaterial flows,
- very good accuracy in case the flow is dominated by transport.

However the disadvantages are also important

- the mesh moves with the flow, so the mesh is somehow an unknown of the problem,
- very often spurious displacements of the mesh is observed. Specific algorithms must be designed with care.
- the mathematical theory of Lagrangian systems of conservation laws show they are often weakly hyperbolic. The theory of weakly hyperbolic systems is not as well understood as the theory of strongly hyperbolic systems [53, 30, 130]. For example the Eulerian systems of compressible gas dynamics is strongly hyperbolic, while the Lagrangian systems of compressible gas dynamics is only weakly hyperbolic.
- perhaps the main difficulty is that one has to change his mind, because the Lagrangian frame is not the observer frame. A detailed analysis shows that the shock relations are the same, but it is not obvious at first examination.

In spite of the huge difficulties attached with Lagrangian numerical methods, their assets are in practice a good reason to use them. We observe that Lagrangian methods are widespread for the numerical simulation of Inertial Confinement flows [99, 16]. Lagrangian schemes for compressible gas dynamics are traditionally staggered methods [13] which have been derived from the seminal work of Von Neumann [109], see [23, 13, 25, 24, 50, 43, 116, 145] and references therein. More recently cell-centered Lagrangian schemes, in the spirit of Godunov's work for which we refer the reader to [54, 55, 139, 86], were derived with the idea of having a compatible discretization. The idea of compatible discretization of partial differential operators is developed in the monograph [131] for example. It can be used in different settings. For example a new approach is the Finite Element formulation of Lagrangian hydrodynamics [127]: this method is by construction staggered and conservative for all physical variables. In the same direction we mention stabilized and variational multiscale formulations for Lagrangian hydrodynamics, see [126, 125, 123, 124], where a globally conservative formulation is obtained from a nodal-based finite element method. The class of method that we present in this section are cell-centered Godunov schemes. We refer to the recent works [38, 39, 97, 99] A summary of recent research on cell-centered Lagrangian methods is developed in [37].

2.2 The Euler-Lagrange change of variable in conservation laws

In this section we detail the algebra of the Euler-Lagrange transformation. To begin with let us consider the two-dimensional Eulerian system of compressible gas dynamics written as a system of conservation laws [53, 130, 30]

$$\begin{cases} \partial_t \rho + \partial_x(\rho u) + \partial_y(\rho v) = 0, \\ \partial_t(\rho u) + \partial_x(\rho u^2 + p) + \partial_y(\rho uv) = 0, \\ \partial_t(\rho v) + \partial_x(\rho uv) + \partial_y(\rho v^2 + p) = 0, \\ \partial_t(\rho e) + \partial_x(\rho ue + pu) + \partial_y(\rho ve + pv) = 0. \end{cases} \quad (2.1)$$

We recast this system on the form $\partial_t U + \partial_x f(U) + \partial_y g(U) = 0$ where the unknown is $U \in \mathbb{R}^4$. Defining $F(U) = (U, f(U), g(U)) \in \mathbb{R}^{4 \times 3}$, the eulerian system (2.1) is also

$$\nabla_{x,y,t} F(U) = 0. \quad (2.2)$$

Of course it is possible to rewrite (2.1) using the convective or material derivative $D_t = \partial_t + u\partial_x + v\partial_y$

$$\begin{cases} \rho D_t \tau - \partial_x u - \partial_y v = 0, \\ \rho D_t u + \partial_x p = 0, \\ \rho D_t v + \partial_y p = 0, \\ \rho D_t e + \partial_x(pu) + \partial_y(pv) = 0. \end{cases} \quad (2.3)$$

This system is very convenient for mechanical interpretation and for the derivation of staggered schemes [13, 145, 121] with artificial viscosity. It is completely equivalent to (2.1) for smooth solutions without shocks. Unfortunately ICF flows contain shocks. In this context the mathematical interpretation of shock solutions to (2.3) is problematic because it is not written in conservative form. This is why it is worthwhile to spend some time to detail other methods available to write Lagrangian formulations. The advantage of these alternative formulations is that they are all conservative, and therefore well suited for a mathematical discussion of shock solutions.

To shorten the notations we set $\mathbf{x} = (x, y)$ and $\mathbf{X} = (X, Y)$. Let us consider the Euler-to-Lagrange change of frame defined by

$$\partial_t \mathbf{x}(\mathbf{X}, t) = u(\mathbf{x}(\mathbf{X}, t), t) \text{ with initialization } \mathbf{x}(\mathbf{X}, 0) = \mathbf{X}. \quad (2.4)$$

Rewriting the eulerian system (2.1) in the Lagrangian frame in function of the variable \mathbf{X} is easy using the algebra of the Piola transformations. We briefly detail the algebra for stationary equations in conservation form. Notice that (2.2) is a space-time conservation equation.

Rule 1 A smooth change of variable $\mathbf{x} \mapsto \mathbf{X}(\mathbf{x})$ is such that $\mathbf{n}d\sigma = \text{cof}(\nabla_{\mathbf{X}}\mathbf{x}) \mathbf{n}_X d\sigma_X$. where $\text{cof}(M) \in \mathbb{R}^{d \times d}$ is the comatrix of M .

Rule 2 A system of conservation laws $\nabla_{\mathbf{x}} F(U) = 0$ written in the eulerian variable is transformed in a lagrangian system written with the \mathbf{X} variable

$$\nabla_{\mathbf{X}} \cdot [F(U) \text{cof}(\nabla_{\mathbf{X}}\mathbf{x})] = 0. \quad (2.5)$$

This is a consequence of rule 1.

Rule 3 One must not forget the Piola's identity

$$\nabla_{\mathbf{X}} \cdot \text{cof}(\nabla_{\mathbf{X}}\mathbf{x}) = 0. \quad (2.6)$$

A reason is that the system (2.5) contains a new unknown $\text{cof}(\nabla_{\mathbf{X}}\mathbf{x})$. Therefore the (2.5) needs new equation to be a closed system (that is a system of conservation laws with the same number of equations and unknowns).

2.2.1 Dimension one

We start from (2.2) and we consider the change of coordinates $(x, t) \mapsto (X, t)$ in \mathbf{R}^2 . The gradient of the space-time transformation is $\begin{pmatrix} 1 & 0 \\ u & J \end{pmatrix}$ with the Jacobian $J = \frac{\partial x}{\partial X}$. The comatrix is $\text{cof} = \begin{pmatrix} J & -u \\ 0 & 1 \end{pmatrix}$. The Lagrangian system (2.5) is

$$\nabla_{x,t} \cdot \left[\begin{pmatrix} \rho & \rho u \\ \rho u & \rho u^2 + p \\ \rho e & \rho e + pu \end{pmatrix} \begin{pmatrix} J & -u \\ 0 & 1 \end{pmatrix} \right] = \partial_t \begin{pmatrix} \rho J \\ \rho J u \\ \rho J e \end{pmatrix} + \partial_X \begin{pmatrix} 0 \\ p \\ pu \end{pmatrix} = 0.$$

The Piola identity (2.6) writes

$$\partial_t J - \partial_X u = 0.$$

It is usual to define the mass variable $dm = \rho(x, t)dx = \rho(X, 0)dX$ which is independent of the time, to eliminate the density $\rho J = \rho(X, 0)$ and to get the system of conservation laws in the mass variable

$$\begin{cases} \partial_t \tau - \partial_m u = 0, \\ \partial_t u + \partial_m p = 0, \\ \partial_t e + \partial_m (pu) = 0. \end{cases} \quad (2.7)$$

Notice that $\rho > 0$ is necessary for the validity of the transformation [144]. The Rankine Hugoniot relations for (2.1) and for (2.7) are physically equivalent.

2.2.2 Dimension two

Our task in this section is to write the Lagrangian equations in dimension two. Let us define for convenience the components of the deformation gradient $\mathbf{F} = \nabla_{\mathbf{X}} \mathbf{x}$ as $A = \partial_X x$, $B = \partial_X y$, $L = \partial_Y x$ and $M = \partial_Y y$.

The algebra of the Euler-Lagrange transformation is as follows. The space-time deformation gradient is $\begin{pmatrix} 1 & 0 & 0 \\ u & A & L \\ v & B & M \end{pmatrix}$. The comatrix is $\text{cof} = \begin{pmatrix} J & -uM + vL & uB - vA \\ 0 & M & -B \\ 0 & -L & A \end{pmatrix}$ where the space Jacobian is $J = AM - BL$. The product of matrices is

$$\begin{pmatrix} \rho & \rho u & \rho v \\ \rho u & \rho u^2 + p & \rho uv \\ \rho v & \rho uv & \rho v^2 + p \\ \rho e & \rho e + pu & \rho e + pv \end{pmatrix} \text{cof} = \begin{pmatrix} \rho J & 0 & 0 \\ \rho u J & pM & -pB \\ \rho v J & -pL & pA \\ \rho e J & puM - pvL & -puB + pvA \end{pmatrix}.$$

So the Eulerian system (2.1) is transformed into the Lagrangian system

$$\begin{cases} \partial_t(\rho J) = 0, \\ \partial_t(\rho J u) + \partial_X(pM) + \partial_Y(-pB) = 0, \\ \partial_t(\rho J v) + \partial_X(-pL) + \partial_Y(pA) = 0, \\ \partial_t(\rho J e) + \partial_X(puM - pvL) + \partial_Y(pvA - puB) = 0. \end{cases} \quad (2.8)$$

The Piola's identities write

$$\begin{cases} \partial_t J - \partial_X(uM - vL) - \partial_Y(vA - uB) = 0, \\ \partial_X M - \partial_Y B = 0, \\ -\partial_X L + \partial_Y A = 0. \end{cases} \quad (2.9)$$

We notice that (2.8-2.9) is not a closed system of conservation laws.

The Hui's system [70] is closed. It writes

$$\begin{cases} \partial_t(\rho J) = 0, \\ \partial_t(\rho J u) + \partial_X(pM) + \partial_Y(-pB) = 0, \\ \partial_t(\rho J v) + \partial_X(-pL) + \partial_Y(pA) = 0, \\ \partial_t(\rho J e) + \partial_X(puM - pvL) + \partial_Y(pvA - puB) = 0, \\ \partial_t A = \partial_X u, \partial_t B = \partial_X v, \partial_t L = \partial_Y u, \partial_t M = \partial_Y v, \quad J = AM - BL. \end{cases} \quad (2.10)$$

A second system proposed in [39] is more concerned with the formal symmetry of the fluxes

$$\begin{cases} \rho_0 \partial_t \tau - \partial_X(uM - vL) - \partial_Y(vA - uB) = 0, & \rho_0 = \rho J, \quad \tau = \frac{1}{\rho}, \\ \rho_0 \partial_t u + \partial_X(pM) + \partial_Y(-pB) = 0, \\ \rho_0 \partial_t v + \partial_X(-pL) + \partial_Y(pA) = 0, \\ \rho_0 \partial_t e + \partial_X(puM - pvL) + \partial_Y(pvA - puB) = 0. \end{cases} \quad (2.11)$$

The third formulation [51] makes use of the Piola-Kirchhoff tensor

$$\sigma^{PK} = \rho_0 \nabla_{\mathbf{F}|S} \varepsilon = \left(\rho_0 \frac{\partial \varepsilon}{\partial \tau |S} \right) \nabla_{\mathbf{F}} \tau = -p \begin{pmatrix} M & -B \\ -L & A \end{pmatrix}.$$

It writes in a compact form

$$\begin{cases} \partial_t \mathbf{F} = \nabla_{\mathbf{X}} \mathbf{u}, \\ \rho_0 \partial_t \mathbf{u} = \nabla_{\mathbf{X}} \cdot \sigma^{PK}, \\ \rho_0 \partial_t e = \nabla_{\mathbf{X}} \cdot (\mathbf{u}^t \sigma^{PK}). \end{cases} \quad (2.12)$$

It is essentially impossible to define simple mass variables in dimension two. If it were possible then they would exist two independent variables (α, β) such that

$$d\alpha = \rho_0 dX \quad \text{and} \quad d\beta = \rho_0 dY.$$

The chain rule implies

$$\partial_\alpha = \frac{\partial X}{\partial \alpha} \partial_X + \frac{\partial Y}{\partial \alpha} \partial_Y = \frac{1}{\rho_0} \partial_X \implies \frac{1}{\rho_0} = \frac{\partial X}{\partial \alpha} \quad \text{and} \quad 0 = \frac{\partial Y}{\partial \alpha}$$

and

$$\partial_\beta = \frac{\partial X}{\partial \beta} \partial_X + \frac{\partial Y}{\partial \beta} \partial_Y = \frac{1}{\rho_0} \partial_Y \implies \frac{1}{\rho_0} = \frac{\partial Y}{\partial \beta} \quad \text{and} \quad 0 = \frac{\partial X}{\partial \beta}.$$

In this case $\frac{\partial \rho^{-1}}{\partial \beta} = \frac{\partial^2 X}{\partial \alpha \partial \beta} = 0$ and $\frac{\partial \rho^{-1}}{\partial \alpha} = \frac{\partial^2 Y}{\partial \alpha \partial \beta} = 0$. So the density ρ is a constant. This is the trivial case. It is not possible to define simple mass variables as in dimension one.

2.2.3 Entropy

The Eulerian system (2.1) is endowed with an entropy inequality

$$\partial_t(\rho S) + \partial_x(\rho u S) + \partial_y(\rho v S) \geq 0 \quad \text{in } \mathcal{D}'_{t,\mathbf{x}}. \quad (2.13)$$

In Lagrange variable it writes

$$\rho_0 \partial_t S \geq 0 \quad \text{in } \mathcal{D}'_{t,\mathbf{X}}. \quad (2.14)$$

These inequalities are in fact equality for smooth solutions.

The algebra is detailed for smooth solution of the third formulation. One has from the fundamental principle of thermodynamics $\rho_0 \partial_t \varepsilon = \rho_0 (T \partial_t S + \nabla_{\mathbf{F}|S} \varepsilon : \partial_t \mathbf{F})$. Therefore

$$\begin{aligned} \rho_0 T \partial_t S &= -\sigma^{PK} : \partial_t \mathbf{F} + \rho_0 \partial_t e - \mathbf{u} \cdot \rho_0 \partial_t \mathbf{u} \\ &= -\sigma^{PK} : \nabla_{\mathbf{X}} \mathbf{u} - \mathbf{u} \cdot \nabla_{\mathbf{X}} \cdot \sigma^{PK} + \nabla_{\mathbf{X}} \cdot (\mathbf{u}^t \sigma^{PK}) = 0. \end{aligned}$$

2.2.4 Hyperbolicity

Hyperbolicity of systems of conservation laws is fundamental property. Assume for simplicity a perfect gas equation of state

$$p = (\gamma - 1) \rho \varepsilon, \quad \gamma > 1, \quad e = \varepsilon + \frac{1}{2} |\mathbf{u}|^2.$$

Then the eulerian system of conservation laws (2.1) is hyperbolic. It means that the Jacobian of the flux has a complete set of real eigenvectors and real eigenvalues. It is a consequence of the fact

that the mathematical entropy $-\rho S$ is a strictly convex functional with respect to the unknowns $(\rho, \rho u, \rho v, \rho e)$ of the eulerian system. The natural definition of the Lagrangian mathematical entropy is of course $-S$. So if $-S$ is a strictly convex functional with respect to the unknowns of one of the Lagrangian systems written above, then this particular Lagrangian system is also hyperbolic. The problem comes from the fact that the size of Lagrangian systems is greater than the size of Eulerian systems. Therefore the strictly hyperbolicity of $-S$ is not guaranteed. Let us detailed this.

In dimension one, the size s of the lagrangian system (2.7) is the same than the original Eulerian system in dimension one, that is $s = 3$. One checks easily that $-S = -\log(\varepsilon\tau^{\gamma-1})$ is strictly convex with respect to τ, u, e . Therefore the lagrangian system (2.7) is hyperbolic.

In dimension two, the situation is less evident because the algebra is tricky and the interpretation of the results may depend on particular version of the lagrangian chosen for the analysis. It has been studied for example in [70, 144, 39]. In all cases the result is that lagrangian systems in dimension greater or equal to two are weakly hyperbolic. A rigorous proof for the system (2.12) is to found in [51]. Perhaps more important is to understand what are the consequences of weak hyperbolicity on the one hand for the solution of the Cauchy problem in dimension two and more, and on the other hand for numerical simulations.

The Cauchy problem of a system of conservation which is only weakly hyperbolic suffers of a loss of derivatives. That is one is able to show stability inequalities in ad-hoc functional spaces like

$$\|U(t)\|_{H^m} \leq C(t) \|U(0)\|_{H^{m+p}}.$$

The integer $p > 0$ measures the number of derivatives which are loosed by the solution of Cauchy problem. Such a phenomenon is characteristic of a weakly hyperbolic system. Let us study a particular Cauchy problem for any lagrangian systems in dimension two. The initial data are

$$p(X, Y, 0) \text{ is a constant, and } u(X, Y, 0) = w(Y), \quad v(X, Y, 0) = 0.$$

The physical solution is of course a pure shear flow

$$x(X, Y, t) = X + tw(Y) \text{ and } y(X, Y, t) = Y.$$

Therefore

$$\mathbf{F}(t) = \begin{pmatrix} 1 & tw'(Y) \\ 0 & 1 \end{pmatrix} = \begin{pmatrix} 1 & t\partial_Y u(0) \\ 0 & 1 \end{pmatrix}$$

So the deformation gradient is a function of the Y derivative of the velocity at time $t = 0$. In consequence the Cauchy problem suffers for the loss of at least one derivative.

The consequence of this weak hyperbolicity for the stability of numerical discretization of Lagrangian equations is not fully understood.

2.3 Schemes in dimension one

In dimension one, it is sufficient to rely on the theory of the solutions to the Riemann problem in order to establish a rigorous and efficient basis for the development of numerical schemes.

The basic scheme that one obtains with this method writes

$$\begin{cases} \frac{M_j}{\Delta t}(\tau_j^{n+1} - \tau_j^n) - u_{j+\frac{1}{2}}^* + u_{j-\frac{1}{2}}^* = 0, \\ \frac{M_j}{\Delta t}(u_j^{n+1} - u_j^n) + p_{j+\frac{1}{2}}^* - p_{j-\frac{1}{2}}^* = 0, \\ \frac{M_j}{\Delta t}(e_j^{n+1} - e_j^n) + p_{j+\frac{1}{2}}^* u_{j+\frac{1}{2}}^* - p_{j-\frac{1}{2}}^* u_{j-\frac{1}{2}}^* = 0. \end{cases} \quad (2.15)$$

where the fluxes are defined by an approximation of the Riemann problem. For example

$$\begin{cases} u_{j+\frac{1}{2}}^* = \frac{1}{2}(u_j^n + u_{j+1}^n) + \frac{1}{2\rho c}(p_j^n - p_{j+1}^n) \\ p_{j+\frac{1}{2}}^* = \frac{1}{2}(p_j^n + p_{j+1}^n) + \frac{\rho c}{2}(u_j^n - u_{j+1}^n). \end{cases}$$

The local acoustic ρc impedance is provided by an approximated formula: for example by $(\rho c)_{j+\frac{1}{2}} = \frac{1}{2} [(\rho c)_j^n + (\rho c)_{j+1}^n]$. More robust and accurate formulas for the local impedance are possible. The mass of cell number j is

$$M_j = \rho_j^0 \Delta x_j^0 = \rho_j^n \Delta x_j^n.$$

The displacement of the cell is defined by

$$x_{j+\frac{1}{2}}^{n+1} = x_{j+\frac{1}{2}}^n + \Delta t u_{j+\frac{1}{2}}^*.$$

It is a enlightening classroom exercise to show that all these formulas are compatible.

2.4 Schemes in dimension 2 or 3

In dimension two the situation is much more complicated. Fortunately there is nowadays a revival of the numerical analysis of multidimensional lagrangian schemes (see references in the introduction of this chapter). In what follows we use the formalism developed in [35]. We detail an abstract derivation of cell-centered lagrangian schemes. It can be proved that this method is compatible with the equations (2.10-2.12). However a fundamental advantage for the practitioner is that it is based on mesh quantities.

In a Lagrangian computation the mesh moves with the flow. The volume of cell j at time $t_k = t_{k-1} + \Delta t$ is denoted as V_j^k . The vertices of the mesh are nodes $\mathbf{x}_r^k \in \mathbb{R}^d$. Let us denote $\mathbf{x}^k = (\mathbf{x}_1^k, \dots, \mathbf{x}_r^k, \dots)$ the collection of all vertices. We assume that the volume V_j^k is defined as a function of the vertices $\mathbf{x}^k \mapsto V_j(\mathbf{x}^k)$. It means that we have a formula to do so, whatever this formula is. In the sequel we concentrate on the consequences of this assumption. We also consider for simplicity the semi-discrete scheme which is continuous in time and fully discrete in space: in this case the volume is $V_j(\mathbf{x}(t))$.

Let us define the gradient of the volume V_j with respect to the nodal positions \mathbf{x}_r

$$\mathbf{C}_{jr} = \nabla_{\mathbf{x}_r} V_j = \left(\frac{\partial}{\partial \mathbf{x}_{r,1}} V_j, \dots, \frac{\partial}{\partial \mathbf{x}_{r,d}} V_j \right)^t \in \mathbb{R}^d. \quad (2.16)$$

In dimension one $V_j = x_{j+\frac{1}{2}} - x_{j-\frac{1}{2}}$. So $\mathbf{C}_{j,j+\frac{1}{2}} = 1$ and $\mathbf{C}_{j,j-\frac{1}{2}} = -1$. Therefore these vectors \mathbf{C}_{jr} are a multidimensional generalization of the notion of an right and left outgoing normal for a lagrangian cell. In dimension two $V_j = \sum_r \frac{1}{2} (x_r y_{r+1} - y_r x_{r+1})$. Therefore the formula (2.16) implies (after elementary manipulations) the formula used in [39]

$$\mathbf{C}_{jr} = \frac{1}{2} (-y_{r-1} + y_{r+1}, x_{r-1} - x_{r+1})^t. \quad (2.17)$$

In any dimension one has by construction

$$\frac{d}{dt} V_j = (\nabla_{\mathbf{x}} V_j, \mathbf{x}') = \sum_r (\mathbf{C}_{jr}, \mathbf{u}_r). \quad (2.18)$$

The Euler relation for homogeneous functions holds, so

$$V_j = \frac{1}{d} (\nabla_{\mathbf{x}} V_j, \mathbf{x}) = \frac{1}{d} \sum_r (\mathbf{C}_{jr}, \mathbf{x}_r). \quad (2.19)$$

For all cell j one has

$$\sum_r \mathbf{C}_{jr} = \mathbf{0}. \quad (2.20)$$

If the vertex \mathbf{x}_r is in the interior of the computational domain and the volumes of the cells are compatible (that is their sum is equal to the total volume) then

$$\sum_j \mathbf{C}_{jr} = \mathbf{0}. \quad (2.21)$$

2.4.1 A nodal solver

The nodal solver is based on two different formulas.

Ingredient 1 We assume a linearized-Riemann-invariant relation in the direction of \mathbf{C}_{jr}

$$p_{jr} - p_j + \rho_j c_j (\mathbf{u}_r - \mathbf{u}_j, \mathbf{n}_{jr}) = 0. \quad (2.22)$$

By definition the normal vector \mathbf{n}_{jr} is such that

$$\mathbf{n}_{jr} = \frac{\mathbf{C}_{jr}}{|\mathbf{C}_{jr}|}, \quad |\mathbf{n}_{jr}| = \sqrt{(\mathbf{n}_{jr}, \mathbf{n}_{jr})} = 1.$$

This relation is an approximation of the Rankine Hugoniot relations for shock hydrodynamics in dimension one, and is commonly used for the design of Godunov solvers.

Ingredient 2 The second formula, needed to construct the nodal solver, expresses that the sum of all forces around the vertex \mathbf{x}_r is zero

$$\sum_j \mathbf{C}_{jr} p_{jr} = 0. \quad (2.23)$$

This formula is natural in the context of Lagrangian methods because it enforces the conservation of momentum.

Solution The solution of the set of equations (2.22-2.23) is easy to compute. Using (2.22) one can eliminate the pressures in (2.23). One gets a linear system

$$\mathbf{A}_r \mathbf{u}_r = \mathbf{b}_r. \quad (2.24)$$

The unknown vector is the node velocity $\mathbf{u}_r \in \mathbb{R}^d$. The matrix is

$$\mathbf{A}_r = \sum_j \rho_j c_j \frac{\mathbf{C}_{jr} \otimes \mathbf{C}_{jr}}{|\mathbf{C}_{jr}|} \in \mathbb{R}^{d \times d}. \quad (2.25)$$

By construction $\mathbf{A}_r = \mathbf{A}_r^t$ is non negative. If the mesh is non degenerate then $\mathbf{A}_r > 0$. Let us be more precise. Assume for example that $\mathbf{A}_r \mathbf{u}_r = 0$, which implies that

$$(\mathbf{u}_r, \mathbf{A}_r \mathbf{u}_r) = \sum_j \rho_j c_j \frac{(\mathbf{C}_{jr}, \mathbf{u}_r)^2}{|\mathbf{C}_{jr}|} = 0 \implies (\mathbf{C}_{jr}, \mathbf{u}_r) = 0 \quad \forall j. \quad (2.26)$$

Due to the equality (2.21) the vectors \mathbf{C}_{jr} are linearly dependent. If the number of these linearly dependent vectors is greater or equal to $d + 1$ then it is enough, in the general case, to generate a basis of \mathbb{R}^d , which implies that $\mathbf{u}_r = 0$. In summary the general case is that if $d + 1$ cells connect to the vertex \mathbf{x}_r , then the matrix \mathbf{A}_r is non-singular. The right hand side is

$$\mathbf{b}_r = \sum_j \mathbf{C}_{jr} p_j + \sum_j \rho_j c_j \frac{\mathbf{C}_{jr} \otimes \mathbf{C}_{jr}}{|\mathbf{C}_{jr}|} \mathbf{u}_j \in \mathbb{R}^d. \quad (2.27)$$

The solution of the linear system is

$$\mathbf{u}_r = \mathbf{A}_r^{-1} \mathbf{b}_r. \quad (2.28)$$

Once the nodal velocities \mathbf{u}_r have been calculated, one computes the nodal pressures p_{jr} using (2.22)

$$p_{jr} = p_j + \rho_j c_j (\mathbf{u}_r - \mathbf{u}_j, \mathbf{n}_{jr}). \quad (2.29)$$

2.4.2 A generic Lagrangian scheme in arbitrary dimension

- 1) At the beginning of the time step one computes the geometrical vectors \mathbf{C}_{jr}^k for all j, r , as a function of the vertices \mathbf{x}_r^k .
- 2) Then one determines the nodal velocities \mathbf{u}_r^k and the nodal pressures p_{jr}^k using the nodal solver (2.28-2.29).

3) It is enough to update the total momentum and the total energy. For the momentum one uses

$$M_j \frac{\mathbf{u}_j^{k+1} - \mathbf{u}_j^k}{\Delta t} = - \sum_r \mathbf{C}_{jr}^k p_{jr}^k. \quad (2.30)$$

The total energy is updated with

$$M_j \frac{e_j^{k+1} - e_j^k}{\Delta t} = - \sum_r (\mathbf{C}_{jr}^k, \mathbf{u}_r^k) p_{jr}^k. \quad (2.31)$$

4) Then the vertices are moved

$$\mathbf{x}_r^{k+1} = \mathbf{x}_r^k + \Delta t \mathbf{u}_r^k \quad (2.32)$$

and one computes the new volume V_j^{k+1} .

5) Finally the new density in the cell is computed

$$\rho_j^{k+1} = \frac{M_j}{V_j^{k+1}} \quad (2.33)$$

2.5 Some numerical results

A lot of hydrodynamic problem can be studied with numerical methods. We give two simple examples that were computed with the method presented above. The first one is a isentropic compression published first by Kidder. The Kidder problem is a strong isentropic compression with a time τ_{foc} of focalisation. It is representative of the smooth isentropic compression of an ICF capsule. The second one is an elementary perturbation problem.

2.5.1 The Kidder problem

We give the result of convergence tests for the Kidder problem [77] in 2D and 3D [98, 26, 35]. To run the problem in a reasonable time in 3D, we use normalized data. A portion of a shell

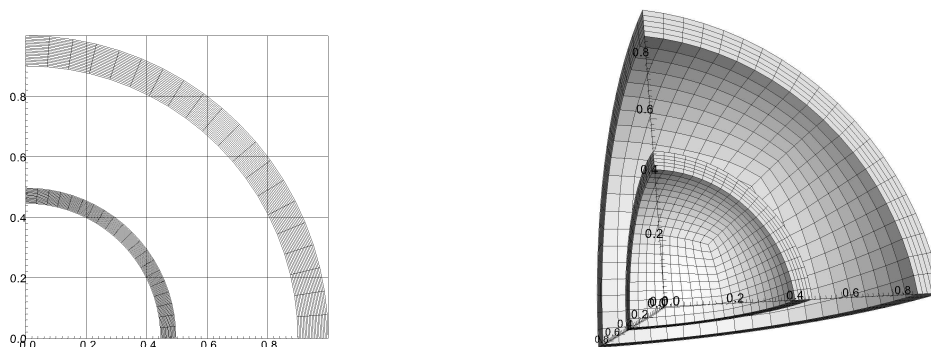


Figure 2.1: Initial condition and final solution for the Kidder problem. 2D on the left, 3D on the right. The data are normalized so that the compression factor is exactly $\frac{1}{2}$ in both cases.

$r_i = 0.9 \leq r \leq 1 = r_e$ is filled with a perfect gas. The adiabatic constant of the gas is $\gamma = 2$ in 2D and $\gamma = \frac{5}{3}$ in 3D. At $t = 0$, the initial density is $\rho_0(r) = \left(\frac{r_e^2 - r^2}{r_e^2 - r_i^2} \rho_i^{\gamma-1} + \frac{r^2 - r_i^2}{r_e^2 - r_i^2} \rho_e^{\gamma-1} \right)^{\frac{1}{\gamma-1}}$, with $\rho_i = 1$ and $\rho_e = 2$. The initial the pressure is $p_0(r) = \rho_0(r)^\gamma$. The initial entropy is uniform $s_0 = \frac{p_0}{\rho_0^\gamma} = 1$. The velocity is $\mathbf{u}_0 = 0$ at $t = 0$. The boundary conditions are: sliding walls on the lateral faces; a given exterior pressure at the internal frontier $p_i(t) = p_0(r_i)h(t)^{-\frac{2\gamma}{\gamma-1}}$; and a given exterior pressure at the external frontier $p_e(t) = p_0(r_e)h(t)^{-\frac{2\gamma}{\gamma-1}}$. Let us denote the sound

speed as c . The solution is known [98] to be an isentropic compression ($s = \frac{p}{\rho^\gamma} = 1$) such that the position at time $t > 0$ is $R(r, t) = h(t)r$, where the compression rate is $h(t) = \sqrt{1 - \frac{t^2}{\tau_{\text{foc}}^2}}$ and the focalisation time is $\tau_{\text{foc}} = \sqrt{\frac{(\gamma-1)(r_e^2 - r_i^2)}{2(c_i^2 - c_e^2)}}$.

In figure 2.1 we display the mesh at $t = 0$ and at the final time of the simulation $t_f = \frac{\sqrt{3}}{2}\tau_{\text{foc}}$, so that the compression rate is $h(t_f) = 0.5$ in both cases. Therefore the analytical solution at t_f is a shell $0.45 \leq R \leq 0.5$. In figure 2.2 we compare the analytical position of the external and internal boundaries with the numerical ones calculated with the low resolution meshes (see below the definition of M_1 and N_1) and with the first order scheme.

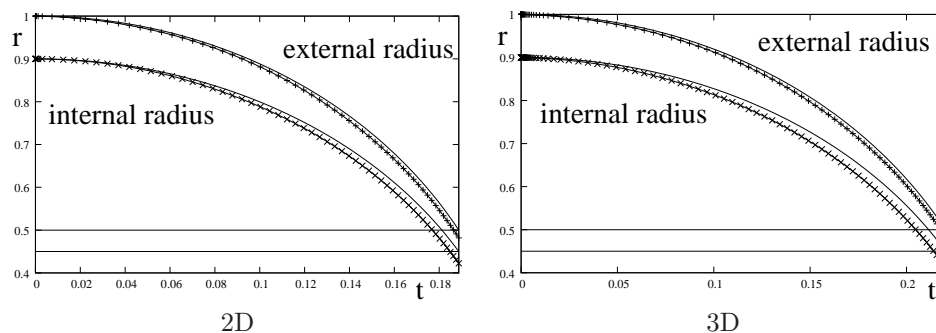


Figure 2.2: The analytical solution is the continuous line, the discrete solution is plotted with symbols. On the left the 2D curves for the mesh M_1 and the first order O_1 scheme. On the right the 3D curves for the mesh N_1 and the order O_1 .

Finally we record in table 2.1 the mean value of the external and internal radii in function of the mesh. In 2D we used four meshes: M_1 is a $10 \times 10 = 100$ cells mesh, that is 10 sectors and 10 layers; M_2 is $20 \times 20 = 400$ cells; M_3 is $40 \times 40 = 1600$ cells; and finally M_4 is $80 \times 80 = 6400$ cells. In 3D we use three meshes: the first mesh N_1 has 10 sectors per facets and 5 layers, since the exterior and interior boundary are designed with 3 square meshes, then the total number of cells is $3 \times 5 \times 10 \times 10 = 1500$ cells; then we double the number of cells in each direction, that N_2 is a 12000 cells mesh; and finally N_3 is a 96000 cells mesh. The order is one (O_1) or two (O_2).

dimension	mesh	order	$r_i(t_f)$	$r_e(t_f)$	order	$r_i(t_f)$	$r_e(t_f)$
2	M_1	O_1	0.4223	0.4820	O_2	0.4343	0.4880
2	M_2	O_1	0.4392	0.4937	O_2	0.4458	0.4966
2	M_3	O_1	0.4453	0.4975	O_2	0.4487	0.4991
2	M_4	O_1	0.4478	0.4989	O_2	0.4495	0.4997
convergence order			≈ 1.09	≈ 1.18		≈ 1.37	≈ 1.58
3	N_1	O_1	0.4133	0.4833	O_2	0.4269	0.4885
3	N_2	O_1	0.4339	0.4929	O_2	0.4422	0.4963
3	N_3	O_1	0.4424	0.4967	O_2	0.4472	0.4987
convergence order			≈ 1.08	≈ 1.10		≈ 1.47	≈ 1.50

Table 2.1: Convergence of the numerical solution towards the exact solution, in function of the order of the scheme (O_1 and O_2) and of the mesh. The order of convergence is systematically computed with the two last meshes in the list (that is M_3M_4 or N_2N_3).

We observe convergence of the numerical solution to the exact one in 2D and 3D. The accuracy of the numerical solution computed with the second order scheme O_2 is similar or better than the accuracy of the O_1 scheme with the mesh just coarser in the list. The experimental order of the convergence is ≈ 1 for O_1 , and is ≈ 1.5 for the second order extension O_2 .

2.5.2 A perturbation problem

ICF flows are very sensitive to hydrodynamic perturbation. That is a even very small initial perturbation may have a dramatic influence on the solution. The reason is that ICF flows are quite close to instability, so that the growth rate of the perturbations may be large. Numerical methods are very useful to quantify the influence these perturbations. Here we illustrate with the result of a very simple numerical simulation done by E. Franck during his Master 2.

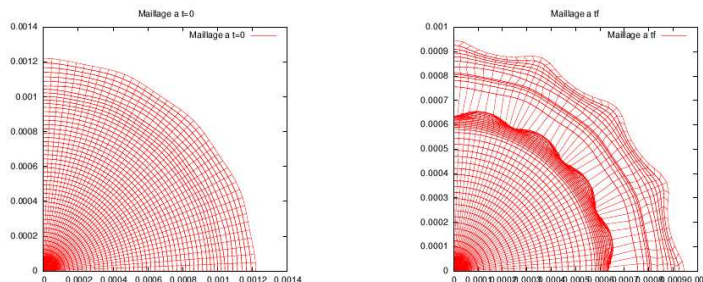


Figure 2.3: The mesh at $t = 0$ is displayed on the left. The perturbation is a $n = 16$ mode. On the right the result at time $t_f = 10^{-9}s$. On this simulation the growth rate of the perturbation is reasonable.

2.6 Numerical analysis

The numerical analysis of Lagrangian is difficult, most probably because of the complexity of such algorithms. One may distinguish between basic conservation formulas, compatibility with the entropy principle and convergence. Compatibility with the entropy principle may be interpreted as a stability principle, but it is not completely clear.

Lemma 2.6.1 *The scheme is conservative in total mass, total momentum and total energy.*

Exercise: Prove this from (2.15) in dimension one, and from (2.23), (2.30) and (2.31) in dimension two.

Lemma 2.6.2 *The semi-discrete scheme is compatible with the entropy principle*

$$S'_j(t) \geq 0.$$

Exercise: Prove this in dimension one from the semi-discrete equations derived from (2.15). In dimension two prove it from (2.18) and the semi-discrete version of (2.30-2.31). A detailed solution is in [35].

The characteristic length of a mesh is h . For the next result we assume that a sequence of meshes, indexed by h , is regular and that the numerical solution is bounded in $BV \cap L^\infty$ [36] independantly of h .

Theorem 2.6.3 [36] *Assume standard regularity assumptions à la Lax. Assume the numerical solution converges in L^1 to some limit as $h \rightarrow 0$. Then the limit is a weak solution to the Euler system (2.1).*

Another assumption is needed to prove the theorem. It writes

$$\sum_r \mathbf{C}_{jr} \otimes \mathbf{x}_r = V_j \mathbf{I}_d.$$

It is true for almost all meshes used in practical simulations. It is in particular true is the volume of the cell can be computed in a way which is compatible with the existence of a reference element.

These properties are also satisfied with the cell-centered schemes developed in [97, 99]. These methods are very close to the one presented above.

2.7 Multi-temperature models

Multi-temperature models are fundamental for the numerical simulation of ICF flows. In what follows we detailed one case, which is concerned with the adaptation in dimension one of the scheme (2.15) to the two temperatures $T_i - T_e$ system (1.2).

The system (1.2) was written in a quasi-Lagrange formulation. So one needs to rewrite in a conservative way. Actually it is possible to do this for the hyperbolic left part of the system. Convenient manipulations of (1.2) give

$$\begin{cases} \partial_t \rho + \partial_x(\rho u) = 0, \\ \partial_t(\rho u) + \partial_x(\rho u^2 + p) = 0, \\ \partial_t(\rho S_e) + \partial_x(\rho u S_e) = 0, \\ \partial_t(\rho e) + \partial_x(\rho u e + pu) = 0, \end{cases} \quad (2.34)$$

where the total energy is $e = \varepsilon_i + \varepsilon_e + \frac{1}{2}u^2$, the total pressure $p = p_i + p_e$ is for simplicity the sum of the ionic pressure $p_i = (\gamma_i - 1)\rho\varepsilon_i$ and of the electronic pressure $p_e = (\gamma_e - 1)\rho\varepsilon_e$. It is easy to show that $-\rho(S_i + S_e)$ is a strictly convex mathematical entropy (this is also the case for $-\rho S_i$). So smooth solutions satisfy $\partial_t(\rho S_i) + \partial_x(\rho u S_i) = 0$. Discontinuous solutions with shocks satisfy

$$\partial_t(\rho S_i) + \partial_x(\rho u S_i) \geq 0. \quad (2.35)$$

As a consequence the ionic entropy increases at shocks while the electronic entropy is constant as shocks

$$S_i^+ > S_i^-, \quad S_e^+ = S_e^-.$$

Exercise: prove it.

This behavior is absolutely fundamental: it explains that ions and electrons behave differently at shocks. In summary physical considerations show that (2.34) is the correct eulerian system of conservation laws to analyze for the two temperature $T_i - T_e$ model.

In Lagrange variable in dimension one, one gets

$$\begin{cases} \partial_t \tau - \partial_m u = 0, \\ \partial_t u + \partial_m p = 0, & p = p_i + p_e, \\ \partial_t S_e = 0, \\ \partial_t e + \partial_m(pu) = 0. \end{cases}$$

Set

$$\rho^2 c_i^2 = -\frac{\partial p_i}{\partial \tau | S_i}, \quad \rho^2 c_e^2 = -\frac{\partial p_e}{\partial \tau | S_e} \text{ and } \rho^2 c^2 = -\frac{\partial p_i}{\tau | S_i} - \frac{\partial p_e}{\tau | S_e}$$

The sound speed of the lagrangian system is ρc where

$$c^2 = c_i^2 + c_e^2. \quad (2.36)$$

Numerical scheme

The natural Lagrangian scheme is now

$$\begin{cases} \frac{M_j}{\Delta t}(\tau_j^{n+1} - \tau_j^n) - u_{j+\frac{1}{2}}^* + u_{j-\frac{1}{2}}^* = 0, \\ \frac{M_j}{\Delta t}(u_j^{n+1} - u_j^n) + p_{j+\frac{1}{2}}^* - p_{j-\frac{1}{2}}^* = 0, \\ (S_e)_j^{n+1} - (S_e)_j^n = 0, \\ \frac{M_j}{\Delta t}(e_j^{n+1} - e_j^n) + p_{j+\frac{1}{2}}^* u_{j+\frac{1}{2}}^* - p_{j-\frac{1}{2}}^* u_{j-\frac{1}{2}}^* = 0. \end{cases} \quad (2.37)$$

The full $T_i - T_e$ system with source terms

A simplified eulerian $T_i - T_e$ system with source terms writes

$$\begin{cases} \partial_t \rho + \partial_x \rho u = 0 \\ \partial_t \rho u + \partial_x(\rho u^2 + p_i + p_e) = 0 \\ \partial_t \rho \varepsilon_i + \partial_x \rho u \varepsilon_i + p_i \partial_x u = \frac{1}{\tau_{ei}}(T_e - T_i) \\ \partial_t \rho \varepsilon_e + \partial_x \rho u \varepsilon_e + p_e \partial_x u = \frac{1}{\tau_{ei}}(T_i - T_e) + \partial_x(K_e \partial_x T_e). \end{cases} \quad (2.38)$$

The relaxation time is τ_{ei} . The electronic diffusion coefficient is K_e . We assume that

$$\varepsilon_i = C_{vi}T_i \text{ et } \varepsilon_e = C_{ve}T_e.$$

As indicated before, a more rigorous way to write this is

$$\begin{cases} \partial_t \rho + \partial_x \rho u = 0 \\ \partial_t \rho u + \partial_x (\rho u^2 + p_i + p_e) = 0 \\ \partial_t \rho S_e + \partial_x \rho u S_e = \frac{1}{\tau_{ei} T_e} (T_i - T_e) + \frac{1}{T_e} \partial_x (K_e \partial_x T_e) \\ \partial_t \rho e + \partial_x (\rho u e + p_i u + p_e u) = \partial_x (K_e \partial_x T_e), \end{cases} \quad (2.39)$$

where the unknowns are the density ρ , the momentum ρu , the electronic entropy ρS_e and the total energy ρe .

Numerical solution based on a splitting strategy

It is very convenient to split the numerical solutions in two stages. The first stage is for the hydrodynamic part, the second stage is for solving the source terms

$$\begin{cases} \partial_t \rho = 0 \\ \partial_t \rho u = 0 \\ \partial_t \rho \varepsilon_i = \frac{1}{\tau_{ei}} (T_e - T_i) \\ \partial_t \rho \varepsilon_e = \frac{1}{\tau_{ei}} (T_i - T_e) + \partial_x (K_e \partial_x T_e). \end{cases} \quad (2.40)$$

It can be done with an implicit linear solver in case the gas is described by perfect gas equations of state.

A simple $T_i - T_e$ numerical result

The numerical simulation displayed in figure 2.4 has been calculated with tabulated coefficients τ_{ei} and K_e . The boundary condition on the right part of the domain is prescribed velocity condition (piston condition). Such a boundary condition is quite reasonable in the context of direct drive. We plot the ionic temperature T_i and the electronic temperature T_e .

We observe that the ionic part of the gas is violently heated because of the shock which propagates from the right to the left. On the other hand the electronic temperature is continuous everywhere. The temperature relaxation is visible behind the shock. In front of the shock a pre-heating phenomenon is visible. This calculation shows the great importance of shocks for ICF flows in the context of direct drive.

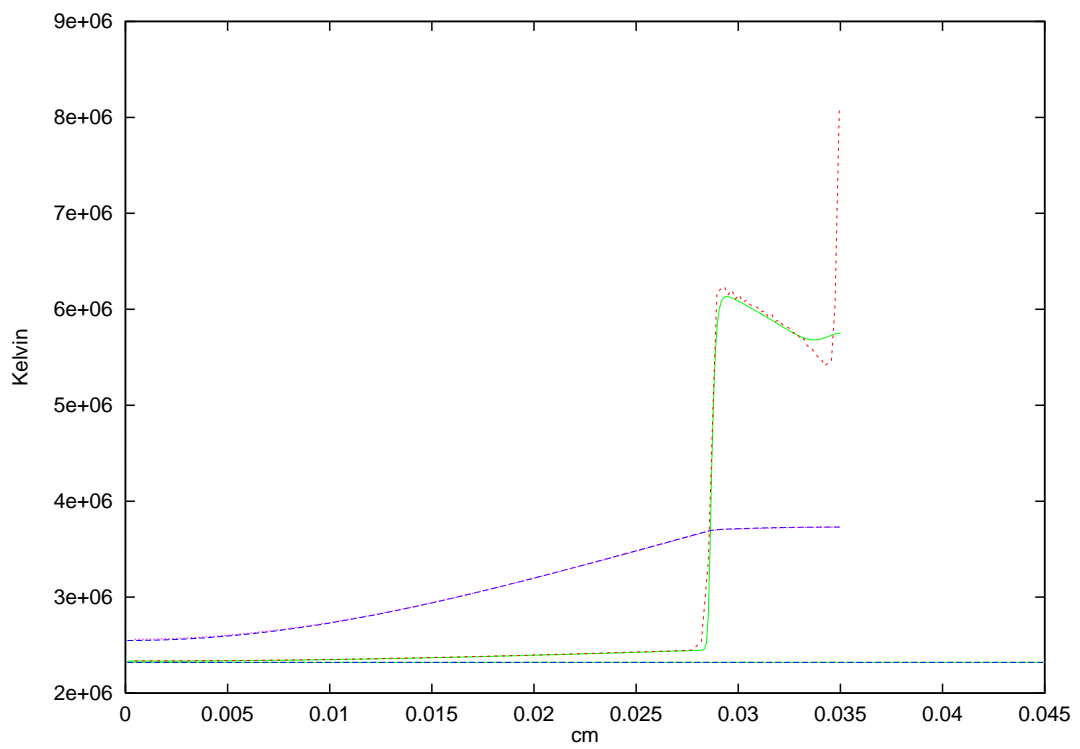


Figure 2.4: The ionic temperature is the discontinuous curve. The electronic temperature is the continuous curve. The initial temperature is the blue curve ($225\,000$ K).

Chapter 3

Radiative transfer

This chapter is devoted to numerical simulations of radiative transfer equation (1.7). More specifically, we are going to focus mainly on the diffusion limit. Then we review theoretical results on these kind of equations, together with some explicit solutions, which are representative of radiative ablation. Special attention is devoted to the diffusion limit and its discretization on distorted meshes. Finally, we also review higher order models, together with asymptotic preserving schemes.

3.1 Radiative transfer equation

We go back to the equation of radiative transfer (1.7), and assume for the sake of simplicity that there is no coupling with hydrodynamics. Using that $\sigma_a = \sigma_e$, the equation thus reads

$$\frac{1}{c} \frac{\partial I_\nu}{\partial t} + \Omega \cdot \nabla I_\nu + \sigma_a(\nu) (I_\nu - B_\nu(T_e)) + \kappa_{\text{Th}} \left(I_\nu - \int_{S^2} \frac{3}{4} \left(1 + (\Omega \cdot \Omega')^2 \right) I_\nu(\Omega') \frac{d\Omega'}{4\pi} \right) = 0, \quad (3.1)$$

where $I_\nu(\mathbf{x}, t, \Omega)$ is the specific radiative intensity, and depends on the space variable \mathbf{x} , the time t , the frequency ν and the direction of propagation $\Omega \in S^2$. In addition to this equation, we need to assume conservation of the energy, namely the last two equations of (1.2), which we rewrite here, assuming that hydrodynamic variables u and ρ are trivial:

$$\frac{\partial E_e}{\partial t} - \text{div}(\chi_e \nabla T_e) + \gamma_{ei}(T_e - T_i) = S + \int_{S^2} \int_0^\infty \sigma_a(\nu) (I_\nu(\mathbf{x}, t, \Omega) - B_\nu(T_e)) d\nu \frac{d\Omega}{4\pi}, \quad (3.2)$$

$$\frac{\partial E_i}{\partial t} - \text{div}(\chi_i \nabla T_i) - \gamma_{ei}(T_e - T_i) = 0 \quad (3.3)$$

In (3.1), (3.2) and (3.3), the coefficients σ_a , κ_{Th} , χ_e , χ_i and γ_{ei} depend on the variables, and in particular on T_e . Therefore, system (3.1)-(3.2)-(3.3) is (highly) nonlinear, even if the equation of state linking (E_e, E_i) with (T_e, T_i) is linear. Let us also recall the value of the Planckian distribution:

$$B_\nu(T) = \frac{2h}{c^2} \frac{\nu^3}{e^{\frac{h\nu}{kT}} - 1}, \quad (3.4)$$

for which we have the equality

$$\int_0^\infty B_\nu(T) d\nu = \frac{ac}{4\pi} T^4, \quad (3.5)$$

where $a = \frac{8\pi^5 k^4}{15h^3 c^3}$ is the black-body constant.

Equation (3.1) is completed by an initial condition I_ν^0 and adapted boundary conditions. These conditions may be of several type (here, \mathcal{D} is the domain of simulation, and for $\mathbf{x} \in \partial\mathcal{D}$, $n(\mathbf{x})$ is the outward normal):

1. Incoming flux condition:

$$\forall \mathbf{x} \in \partial\mathcal{D}, \quad \forall \Omega / \Omega \cdot \mathbf{n}(\mathbf{x}) \leq 0, \quad I_\nu(\mathbf{x}, t, \Omega) = I_\nu^{\text{ext}}(\mathbf{x}, t, \Omega), \quad (3.6)$$

for some given function I_ν^{ext} .

2. Albedo conditions:

$$\forall \mathbf{x} \in \partial\mathcal{D}, \quad \forall \Omega / \Omega \cdot \mathbf{n}(\mathbf{x}) \leq 0, \quad I_\nu(\mathbf{x}, t, \Omega) = \frac{1-\omega}{2\pi} \int_{\Omega' \cdot \mathbf{n} > 0} I_\nu(\mathbf{x}, t, \Omega') d\Omega', \quad (3.7)$$

where $\omega \in [0, 1]$ is the albedo coefficient.

3. Reflexion conditions:

$$\forall \mathbf{x} \in \partial\mathcal{D}, \quad \forall \Omega / \Omega \cdot \mathbf{n}(\mathbf{x}) \leq 0, \quad I_\nu(\mathbf{x}, t, \Omega) = I_\nu(\mathbf{x}, t, \Omega - 2(\Omega \cdot \mathbf{n})\mathbf{n}). \quad (3.8)$$

In equation (3.1), the mean free path is equal to

$$\lambda = \frac{1}{\sigma_a + \kappa_{\text{Th}}}.$$

As mentioned in the introduction, treating (3.1) in its full generality is for now not possible, since it amounts to discretizing the variables $(\mathbf{x}, t, \Omega, \nu) \in \mathbb{R}^3 \times \mathbb{R}^+ \times S^2 \times \mathbb{R}^+$. However, two limit cases can be identified in which (3.1) can be replaced by simpler equations. These two regimes correspond to the free streaming limit in which λ is large, and the diffusion limit in which λ is small. In the first case, the materials we deal with are transparent, whereas in the second case, they are opaque.

3.1.1 Free streaming limit

This regime is justified if λ is small compared to the variation of the radiative energy density, that is,

$$\lambda = \frac{1}{\sigma_a(\nu) + \kappa_{\text{Th}}} \ll \frac{I_\nu}{|\nabla I_\nu|}, \quad \text{and} \quad \tau = \frac{\lambda}{c} \ll \frac{I_\nu}{\left| \frac{\partial I_\nu}{\partial t} \right|}. \quad (3.9)$$

In this limit, the equation is close to the free streaming equation, that is,

$$\frac{\partial I}{\partial t} + c\Omega \cdot \nabla I = 0.$$

An efficient method for simulating such an equation is Monte Carlo method. We do not develop this aspect here, and refer to [34] and [79] for details.

3.1.2 Diffusion limit

This regime corresponds to the hypothesis that

$$\lambda = \frac{1}{\sigma_a(\nu) + \kappa_{\text{Th}}} \gg \frac{I_\nu}{|\nabla I_\nu|}, \quad \text{and} \quad \tau = \frac{\lambda}{c} \gg \frac{I_\nu}{\left| \frac{\partial I_\nu}{\partial t} \right|}. \quad (3.10)$$

Note that this may happen either if σ_a is large, or if κ_{Th} is large. We consider in the present case the second possibility. In such a case, the radiative energy density is almost isotropic, hence we assume that a good approximation is given by

$$I_\nu(\Omega) = \frac{1}{4\pi} cE_\nu + \frac{3}{4\pi} \Omega \cdot F_\nu, \quad (3.11)$$

where E_ν and F_ν are independent of Ω , and are thus equal to the first and second moment of I_ν , respectively:

$$E_\nu = \frac{1}{c} \int_{S^2} I_\nu(\Omega) d\Omega, \quad F_\nu = \int_{S^2} \Omega I_\nu(\Omega) d\Omega. \quad (3.12)$$

Hence, taking the first and second moment of equation (3.1), one gets:

$$\begin{cases} \frac{\partial E_\nu}{\partial t} + \operatorname{div}(F_\nu) + c\sigma_a(\nu) \left(E_\nu - \frac{4\pi}{c} B_\nu(T_e) \right) = 0, \\ \frac{1}{c} \frac{\partial F_\nu}{\partial t} + \frac{c}{3} \nabla E_\nu + (\sigma_a(\nu) + \kappa_{\text{Th}}) F_\nu = 0. \end{cases} \quad (3.13)$$

This system is usually called the "P1 system", since we have used a P1 approximation of I as a function of Ω to obtain it. In order to simplify further (3.13), we also use a non-relativistic hypothesis: assuming that $|\partial_t I_\nu|/|\nabla I_\nu| \ll c$, we infer that $|\partial_t F_\nu| \ll c^2 |\nabla E_\nu|$. This simplifies the second line of (3.13) into

$$F_\nu = -\frac{c}{3(\sigma_a(\nu) + \kappa_{\text{Th}})} \nabla E_\nu, \quad (3.14)$$

so that we finally have

$$\frac{\partial E_\nu}{\partial t} - \operatorname{div} \left(\frac{c}{3(\sigma_a(\nu) + \kappa_{\text{Th}})} \nabla E_\nu \right) + c\sigma_a(\nu) \left(E_\nu - \frac{4\pi}{c} B_\nu(T_e) \right) = 0. \quad (3.15)$$

Note that (3.15) is drastically different in nature from (3.13). Indeed, (3.13) is hyperbolic, hence exhibits finite propagation speed, whereas (3.15) is parabolic, and thus has infinite speed propagation.

Let us point out that the definition (3.12) implies that

$$|F_\nu| \leq cE_\nu,$$

a condition which is clearly not ensured by equality (3.14). Therefore, when such a condition is violated, one usually uses flux limitors in order to restore it [105, 114, 87, 140, 88, 107]. We will come back to this issue in Section 3.2 below.

3.1.3 Boundary conditions in the diffusion limit

Equation (3.15) should be complemented by adapted boundary conditions. However, conditions (3.6), (3.7) and (3.8) are not easily adapted to diffusion boundary conditions. Let us give the example of incoming flux boundary condition (3.6): we multiply this equation by $|\Omega \cdot \mathbf{n}|$ and integrate over the half sphere $\Omega \cdot \mathbf{n} \leq 0$, finding

$$\int_{\Omega \cdot \mathbf{n} \leq 0} |\Omega \cdot \mathbf{n}| I_\nu(\mathbf{x}, t, \Omega) d\Omega = \int_{\Omega \cdot \mathbf{n} \leq 0} |\Omega \cdot \mathbf{n}| I_\nu^{\text{ext}}(\mathbf{x}, t, \Omega) d\Omega := F_\nu^{\text{in}}(\mathbf{x}, t),$$

where F_ν^{in} is the incoming flux, and is a datum. Then, we use (3.11), together with (3.14), finding

$$\frac{c}{4\pi} E_\nu \int_{\Omega \cdot \mathbf{n} \leq 0} |\Omega \cdot \mathbf{n}| d\Omega + \frac{3}{4\pi} \left(-\frac{c \nabla E_\nu}{3(\sigma_a(\nu) + \kappa_{\text{Th}})} \right) \cdot \int_{\Omega \cdot \mathbf{n} \leq 0} |\Omega \cdot \mathbf{n}| \Omega d\Omega = F_\nu^{\text{in}}.$$

Hence,

$$E_\nu + \frac{2}{3(\sigma_a(\nu) + \kappa_{\text{Th}})} \frac{\partial E_\nu}{\partial n} = \frac{4}{c} F_\nu^{\text{in}}. \quad (3.16)$$

This boundary condition is usually referred to as "Marshak boundary condition". The quantity $\ell = \frac{2}{3(\sigma_a(\nu) + \kappa_{\text{Th}})}$ is called the extrapolation length.

It is of course important to know the validity of this approximation. We have seen that a good criterion is (3.10) for (3.15) to hold. As far as (3.16) is concerned, one may argue that the following inequality should hold:

$$F_\nu^{\text{out}}(\mathbf{x}, t) := \int_{\Omega \cdot \mathbf{n} \geq 0} |\Omega \cdot \mathbf{n}| I_\nu(\mathbf{x}, t, \Omega) d\Omega \geq 0.$$

Hence, using (3.11) and (3.14) again in this inequality, we find

$$E_\nu - \frac{2}{3(\sigma_a + \kappa_{\text{Th}})} \frac{\partial E_\nu}{\partial \mathbf{n}} \geq 0. \quad (3.17)$$

This condition gives an indication about the validity of boundary condition (3.16).

Condition (3.16) may be a poor approximation in some situations. Indeed, if the incoming flux is not isotropic, since by nature the radiative intensity I_ν is isotropic, the solution of (3.1) will develop a boundary layer. This boundary layer is not taken into account here. A possibility is to carry out an asymptotic analysis in order to compute it properly, and then use it to derive an adapted boundary condition. We refer to [29, 128, 57] for more details on this subject.

3.2 Mathematical analysis

3.2.1 Existence results for the radiative transfer equation

The original system of radiative transfer (3.1) coupled with an energy equation similar to (3.2)-(3.3) (that is, (3.2)-(3.3) with $T_e = T_i$), was proved to be well posed in [103] and [56]. These results have been improved by [94], and more recently by [115]. Let us cite here main result of [56]:

Theorem 3.2.1 (F. Gorse, B. Perthame, [56]) *Assume that \mathcal{D} is a smooth convex domain of \mathbb{R}^3 , that $T_e = T_i = T$ and $\chi_e = \chi_i = 0$ and $S = 0$ in (3.2)-(3.3), which are therefore replaced by*

$$C_\nu \frac{\partial T}{\partial t} = \int_{S^2} \int_0^\infty \sigma_a(\nu) (I_\nu(\mathbf{x}, t, \Omega) - B_\nu(T)) d\nu \frac{d\Omega}{4\pi}, \quad (3.18)$$

where we have assumed perfect gas equation of state. Assume in addition that the following assumptions hold:

- (i) $\sigma_a(\nu, T) > 0$ for all $\nu > 0$ and $T > 0$;
- (ii) $\forall \nu > 0$, $T \mapsto \sigma_a(\nu, T)$ is of class C^1 in $(0, \infty)$;
- (iii) $\forall \nu > 0$, $T \mapsto \sigma_a(\nu, T)$ is nonincreasing, and $T \mapsto \sigma_a(\nu, T)B_\nu(T)$ is nondecreasing;
- (iv) $\forall \nu > 0$, $\sigma_a(\nu, T)B_\nu(T) \rightarrow 0$ as $T \rightarrow 0$;
- (v) the application $T \mapsto \sigma_a(\nu, T)B_\nu(T)$ is continuous from $L^1(\mathcal{D})$ to $L^1(\mathcal{D} \times (0, \infty))$;
- (vi) the boundary condition I^{ext} in (3.6) satisfies $0 \leq I_\nu^{\text{ext}}(\mathbf{x}, t, \Omega) \leq B_\nu(T^{\text{ext}})$, for some fixed $T^{\text{ext}} > 0$, and
- (vii) the initial conditions (I^0, T^0) are in $L^1(\mathcal{D}) \times L^1(\mathcal{D} \times S^2 \times (0, \infty))$.

Then, problem (3.1)-(3.18) with boundary condition (3.6) and initial condition (I^0, T^0) has a global mild solution.

In addition, if there exists $T_{\text{max}} > 0$ (respectively $T_{\text{min}} > 0$) such that

$$\left\{ \begin{array}{l} T^0 \leq T_{\text{max}}, \\ I^0 \leq B_\nu(T_{\text{max}}), \\ I^{\text{ext}} \leq B_\nu(T_{\text{max}}), \end{array} \right. \left(\text{respectively} \left\{ \begin{array}{l} T^0 \geq T_{\text{min}}, \\ I^0 \geq B_\nu(T_{\text{min}}), \\ I^{\text{ext}} \geq B_\nu(T_{\text{min}}), \end{array} \right. \right)$$

then we have

$$\forall \mathbf{x} \in \mathcal{D}, \forall t > 0, \left\{ \begin{array}{l} T \leq T_{\text{max}}, \\ I \leq B_\nu(T_{\text{max}}), \end{array} \right. \left(\text{respectively} \left\{ \begin{array}{l} T \geq T_{\text{min}}, \\ I \geq B_\nu(T_{\text{min}}). \end{array} \right. \right)$$

We refer to [56] for the details, and in particular for the notion of mild solutions.

Some comments are in order about this result.

First, it is pointed out in [56] that assumption (vi) on the boundary condition is not necessary for the above result to hold, and that a sufficient condition is

$$\int_{\partial\mathcal{D}} \int_{\Omega \cdot \mathbf{n} < 0} \int_0^\infty |I_\nu^{\text{ext}}| |\Omega \cdot \mathbf{n}| d\nu d\Omega d\mathbf{x} < \infty.$$

However, (vi) is physically relevant and allows for finer regularity results.

Second, some regularity results are also given in [56] under additional assumptions. In particular, BV bounds are proved.

Third, the same kind of result is proved in [115], still with $T_e = T_i$ and a perfect gas equation of state, but with a diffusion coefficient $\chi = \chi_e + \chi_i \neq 0$.

Finally, we point out that hypothesis (iii) is not physically relevant [28, 104, 112, 11], but allows to prove accretiveness of the semi-group associated to (3.1). When dropping such an assumption, the same result is only proved for a simpler system [11].

3.2.2 Rigorous justification of the diffusion limit

In Subsection 3.1.2, we have given a formal justification for the diffusion limit of (3.1). We are now going to give a more explicit derivation based on Hilbert expansion. We are thus lead to finding a limit in which (3.1) does converge in a certain mathematical sense to (3.15). For this purpose, a common assumption is that the unknowns (energy and temperature) vary slowly in time and space. This is equivalent to using a rescaling [80, 128, 11] of the form

$$t \mapsto \varepsilon^2 t, \quad \mathbf{x} \mapsto \varepsilon \mathbf{x}, \quad (3.19)$$

where ε is a small parameter. This kind of assumption was also present in a different form in [112, 44, 100, 117]. Therefore, we are lead to study the following equation:

$$\begin{aligned} \frac{\varepsilon}{c} \frac{\partial I_\nu}{\partial t} + \Omega \cdot \nabla I_\nu + \frac{\sigma_a(\nu)}{\varepsilon} (I_\nu - B_\nu(T)) \\ + \frac{\kappa_{\text{Th}}}{\varepsilon} \left(I_\nu - \int_{S^2} \frac{3}{4} \left(1 + (\Omega \cdot \Omega')^2 \right) I_\nu(\Omega') \frac{d\Omega'}{4\pi} \right) = 0, \end{aligned} \quad (3.20)$$

in the limit $\varepsilon \rightarrow 0$. Here, we have set $T = T_e = T_i$ in order to simplify the problem. Assuming in addition a perfect gas equation of state, the energy conservation for matter is thus (3.18), which we recall here:

$$\varepsilon C_v \frac{\partial T}{\partial t} = \int_{S^2} \int_0^\infty \frac{\sigma_a(\nu)}{\varepsilon} (I_\nu(\mathbf{x}, t, \Omega) - B_\nu(T)) d\nu \frac{d\Omega}{4\pi} \quad (3.21)$$

The following theorem was proved in [80] and [10] (see also [11, 12]):

Theorem 3.2.2 (Diffusion approximation, [80, 10]) *Assume the hypotheses of Theorem 3.2.1 are satisfied, and that*

$$\exists p > 1, \quad \exists C > 0, \quad \exists \sigma_m > 0, \quad \exists \theta > 0, \quad \forall T \in (0, \theta), \quad \forall \nu > 0, \quad \sigma_m \leq \sigma_a(\nu, T) \leq CT^{-1/p}. \quad (3.22)$$

Let $(I_\nu^\varepsilon, T^\varepsilon) \in C^0(\mathbb{R}^+, L^1(\mathcal{D} \times \mathbb{R}^+ \times S^2)) \times C^0(\mathbb{R}^+, L^2(\mathcal{D}))$ be the unique solution of (3.20)-(3.21), with boundary conditions (3.6), with

$$I_\nu^{\text{ext}}(\mathbf{x}, t, \Omega) = B_\nu(T^{\text{ext}}(\mathbf{x}, t)),$$

where T^{ext} is the boundary condition for (3.21), and with initial conditions

$$I_\nu^0(\mathbf{x}, \Omega) = B_\nu(T^0(\mathbf{x})),$$

where T^0 is the initial condition for (3.21). Assume in addition that the compatibility condition $T^{\text{ext}}(\mathbf{x}, 0) = T^0(\mathbf{x})$ is satisfied on $\partial\mathcal{D}$. Then up to extracting a subsequence, we have the convergences, for any $t^* > 0$:

$$\begin{cases} T^\varepsilon \xrightarrow{\varepsilon \rightarrow 0} T & \text{in } L^2((0, t^*) \times \mathcal{D}), \\ I_\nu^\varepsilon \xrightarrow{\varepsilon \rightarrow 0} B_\nu(T) & \text{in } L^2((0, t^*) \times \mathcal{D} \times S^2 \times \mathbb{R}^+), \end{cases}$$

where T is the unique solution of the Rosseland equation:

$$\frac{1}{c} \frac{\partial}{\partial t} (C_v T + acT^4) - \text{div} \left(\frac{1}{3\sigma_R(T)} \nabla (acT^4) \right) = 0, \quad (3.23)$$

where

$$\frac{1}{\sigma_R(T)} = \left(\int_0^\infty B'_\nu(T) d\nu \right)^{-1} \int_0^\infty \frac{B'_\nu(T)}{\sigma_a(\nu, T) + \kappa_{\text{Th}}} d\nu, \quad (3.24)$$

and T satisfies the same boundary and initial conditions as T^ε .

We do not give the complete proof of this result here, but the Hilbert expansion argument: we assume that

$$\begin{aligned} I_\nu &= I^0 + \varepsilon I^1 + \varepsilon^2 I^2 + \dots, \\ T &= T^0 + \varepsilon T^1 + \varepsilon^2 T^2 + \dots \end{aligned}$$

Inserting these expansions into (3.20) - (3.21), and identifying the corresponding powers of ε , we find:

order ε^{-1} :

$$\sigma_a(\nu) (I_\nu^0 - B_\nu(T^0)) + \kappa_{\text{Th}} (I_\nu^0 - \mathcal{K}(I_\nu^0)) = 0, \quad (3.25)$$

where we have denoted by \mathcal{K} the Thomson scattering operator, namely

$$\mathcal{K}(I)(\Omega) = \int_{S^2} \frac{3}{4} \left(1 + (\Omega \cdot \Omega')^2 \right) I(\Omega') \frac{d\Omega'}{4\pi}.$$

Here we point out that the spectrum of the operator \mathcal{K} is included in $[0, 1]$ (see Lemma 3.2.4 below). Hence, rewriting (3.25) as

$$\frac{\sigma_a(\nu) + \kappa_{\text{Th}}}{\kappa_{\text{Th}}} I_\nu^0 - \mathcal{K}(I_\nu^0) = \sigma_a(\nu) B_\nu(T^0),$$

it is clear that it has at most one solution. Since $B_\nu(T^0)$ is a solution, we infer

$$I_\nu^0 = B_\nu(T^0). \quad (3.26)$$

order ε^0 :

$$\Omega \cdot \nabla I_\nu^0 + \sigma_a(\nu) (I_\nu^1 - B'_\nu(T^0)T^1) + \kappa_{\text{Th}} (I_\nu^1 - \mathcal{K}(I_\nu^1)) = 0. \quad (3.27)$$

We divide this equation by $\sigma_a + \kappa_{\text{Th}}$, take its gradient and multiply by Ω . Integrating the result with respect to Ω , we have

$$\int_{S^2} \Omega \cdot \nabla I_\nu^1(\mathbf{x}, t, \Omega) d\Omega = -4\pi \text{div} \left(\frac{1}{3(\sigma_a(\nu) + \kappa_{\text{Th}})} \nabla I_\nu^0 \right). \quad (3.28)$$

order ε^1 :

$$\frac{1}{c} \frac{\partial I_\nu^0}{\partial t} + \Omega \cdot \nabla I_\nu^1 + \sigma_a(\nu) \left(I_\nu^2 - B'_\nu(T^0)T^2 - B''_\nu(T^0) \frac{(T^1)^2}{2} \right) + \kappa_{\text{Th}} [I_\nu^2 - \mathcal{K}(I_\nu^2)] = 0, \quad (3.29)$$

and

$$C_v \frac{\partial T^0}{\partial t} = \int_{S^2} \int_0^\infty \sigma_a(\nu) \left(I_\nu^2(\mathbf{x}, t, \Omega) - B'_\nu(T^0)T^2 - B''_\nu(T^0) \frac{(T^1)^2}{2} \right) d\Omega d\nu = 0. \quad (3.30)$$

Integrating (3.29) with respect to Ω and ν , and summing the result with (3.30), we find

$$\frac{1}{c} \frac{\partial}{\partial t} (C_\nu T^0 + ac(T^0)^4) + \int_{S^2} \int_0^\infty \Omega \cdot \nabla I^1(\mathbf{x}, t, \Omega) d\nu \frac{d\Omega}{4\pi},$$

which, with the help of (3.28), gives (3.23).

The above computations, although formal, give the main lines of the proof of Theorem 3.2.2. We refer to [10] for the details.

We then point out that the above argument is clearly also valid if one starts from the diffusion approximation (3.15) instead of (3.20). Actually, the technical details of the proof are even simpler. We therefore may state the following result:

Theorem 3.2.3 *Under the hypotheses of Theorem 3.2.2, if $(E_\nu^\varepsilon, T^\varepsilon)$ is a solution to the system (3.15)-(3.21), that is,*

$$\begin{cases} \frac{\varepsilon}{c} \frac{\partial E_\nu}{\partial t} - \operatorname{div} \left(\frac{1}{3(\sigma_a(\nu) + \kappa_{\text{Th}})} \nabla E_\nu \right) + \frac{\sigma_a(\nu)}{\varepsilon} \left(E_\nu - \frac{4\pi}{c} B_\nu(T_\varepsilon) \right) = 0, \\ \varepsilon C_\nu \frac{\partial T}{\partial t} = \frac{c}{4\pi} \int_0^\infty \frac{\sigma_a(\nu)}{\varepsilon} \left(E_\nu(\mathbf{x}, t) - \frac{4\pi}{c} B_\nu(T) \right) d\nu, \end{cases} \quad (3.31)$$

with the same form of boundary and initial conditions as in Theorem 3.2.2. Then, up to extracting a subsequence, we have the convergences, for any $t^* > 0$,

$$\begin{cases} T^\varepsilon \xrightarrow{\varepsilon \rightarrow 0} T & \text{in } L^2((0, t^*) \times \mathcal{D}), \\ E_\nu^\varepsilon \xrightarrow{\varepsilon \rightarrow 0} B_\nu(T) & \text{in } L^2((0, t^*) \times \mathcal{D} \times \mathbb{R}^+), \end{cases}$$

where T is the unique solution of the Rosseland equation (3.23).

Hence, gathering the results of Theorem 3.2.2 and Theorem 3.2.3, we see that the model (3.31) is a good approximation of the radiative transfer model. This gives a rigorous justification for the use of (3.31). This model takes into account the fact that in ICF experiments, radiation is almost isotropic, whereas its spectrum may be different from a Planckian distribution.

Another way to justify rigorously the model (3.31) is to use a different scaling of the coefficients in (3.20), namely

$$\frac{\varepsilon}{c} \frac{\partial I_\nu}{\partial t} + \Omega \cdot \nabla I_\nu + \varepsilon \sigma_a(\nu) (I_\nu - B_\nu(T)) + \frac{\kappa_{\text{Th}}}{\varepsilon} \left(I_\nu - \int_{S^2} \frac{3}{4} (1 + (\Omega \cdot \Omega')^2) I_\nu(\Omega') \frac{d\Omega'}{4\pi} \right) = 0.$$

This correspond to assuming, in addition to the scaling (3.19), that $\sigma_a \propto \varepsilon^2 \kappa_{\text{Th}}$. Then, an asymptotic analysis gives, as a limit model, (3.31), but with a different diffusion coefficient, namely

$$\chi_r = \frac{1}{3\kappa_{\text{Th}}}.$$

Such an analysis is presented in [21]. Finally, in order to justify the actual value of the diffusion coefficient in (3.31), one argues that the hypothesis on σ_a and κ_{Th} imply $\kappa_{\text{Th}} \approx \kappa_{\text{Th}} + \sigma_a$.

Note that in the above derivation, we have deliberately left aside the question of boundary layer in the diffusion approximation. For this, we refer to [128] and [57], simply pointing out that if the boundary condition is not Planckian, then one needs to compute a boundary layer, that is, assume a solution of the form

$$I_\nu^\varepsilon(\mathbf{x}, t, \Omega) = I_\nu^0 \left(\frac{\mathbf{x} \cdot \mathbf{n}}{\varepsilon}, \mathbf{x}, t, \Omega \right) + \varepsilon I_\nu^1 \left(\frac{\mathbf{x} \cdot \mathbf{n}}{\varepsilon}, \mathbf{x}, t, \Omega \right) + \dots,$$

near the boundary, where n is the outward normal to the boundary. Inserting this kind of expansion into the radiative transfer equation, and using the same kind of computation as above, one is lead

to study Milne's problem in order to derive a boundary condition for Rosseland equation (3.23). Details for this may be found in [128, 57, 29].

We give now the proof of the following, which was used in the sketch of the proof of Theorem 3.2.2:

Lemma 3.2.4 *Consider the Thomson operator \mathcal{K} , defined by*

$$\mathcal{K}(I) = \frac{3}{4} \int_{S^2} (1 + (\Omega \cdot \Omega')^2) I(\Omega') \frac{d\Omega'}{4\pi}.$$

This operator is a bounded operator self-adjoint operator on $L^2(S^2)$, its spectrum consists of a finite set of eigenvalues, is included in $[0, 1]$, and 1 is a simple eigenvalue of \mathcal{K} , with eigenvector $I = 1$.

Proof: it is clear that \mathcal{K} is bounded. In addition, applying Fubini's Theorem, one easily proves that it is self-adjoint. Moreover, it is clear that $\text{Ran}(\mathcal{K})$ is included into the space of polynomial of degree lower than 2 in Ω , which is of finite dimension. Hence, its spectrum consists of a finite set of eigenvalues. Further, $\mathcal{K}(1) = 1$, and, if (λ, I) is an eigenpair of \mathcal{K} , with $\int I = 0$, we have

$$\lambda I = \mathcal{K}(I) = \frac{3}{4} \int_{S^2} (\Omega \cdot \Omega')^2 I(\Omega') \frac{d\Omega'}{4\pi}.$$

We then compute, denoting by $\langle \cdot, \cdot \rangle$ the scalar product of $L^2(S^2)$, and $\|\cdot\|$ the corresponding norm,

$$\begin{aligned} \lambda \|I\|^2 &= \langle \mathcal{K}(I), I \rangle = \frac{3}{16\pi} \int_{S^2} \int_{S^2} (\Omega \cdot \Omega')^2 I(\Omega') I(\Omega) d\Omega' d\Omega \\ &= \frac{3}{16\pi} \sum_{i=1}^3 \sum_{j=1}^3 \int_{S^2} \Omega_i \Omega_j I(\Omega) d\Omega \int_{S^2} \Omega'_i \Omega'_j I(\Omega') d\Omega' = \frac{3}{16\pi} \sum_{i=1}^3 \sum_{j=1}^3 \left(\int_{S^2} \Omega_i \Omega_j I(\Omega) d\Omega \right)^2 \geq 0, \end{aligned}$$

and

$$\langle \mathcal{K}(I), I \rangle = \frac{3}{16\pi} \int_{S^2} \int_{S^2} (\Omega \cdot \Omega')^2 I(\Omega') I(\Omega) d\Omega' d\Omega \leq \frac{3}{16\pi} \left(\int_{S^2} I \right)^2 \leq \frac{3}{4} \|I\|^2,$$

where we have used Cauchy-Schwarz inequality. This proves that $\lambda \in [0, 3/4]$, which implies that $\lambda = 1$ is a simple eigenvalue. \square

3.2.3 Marshak waves

Now that we have asserted the the validity of the model (3.31), or its equivalent three-temperature model, that is, (3.15) coupled with (3.2)-(3.3), let us give a few words about qualitative behaviour of solutions to such a system.

In order to do so, and since we are only interested here in *qualitative* behaviour, we are going to simplify the system. Indeed, the main feature of (3.31) is that it is a nonlinear diffusion equation, which is already the case of (3.23). One may thus expect that it is sufficient to study (3.23). Still, let us simplify further this model in order to be able to carry out explicit computations: we study the equation

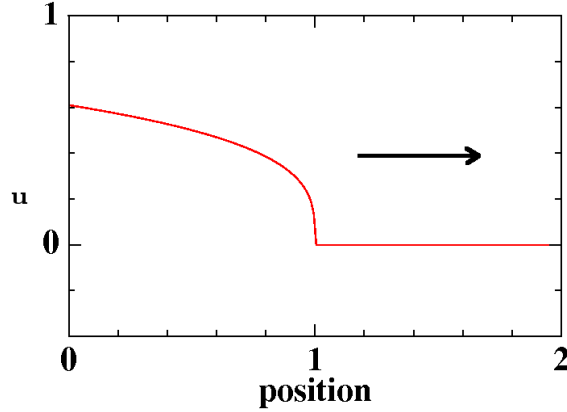
$$\frac{\partial u}{\partial t} - \text{div}(u^m \nabla u) = 0, \quad (3.32)$$

for some constant $m > 0$. This crude approximation is justified by the fact that $\sigma_R(T)$, for T large, behaves like a power of T [104]. We look for non-negative solutions u of (3.32) on the whole space. Such an equation has been extensively studied, especially in link with flow in porous media [83, 6, 7, 110, 78, 76, 18, 8, 142]. It is well known that one can compute explicit solutions which are travelling wave. Indeed, looking for solutions of the form

$$u(\mathbf{x}, t) = (ct - x_i)_+^\alpha, \quad (3.33)$$

where $c \in \mathbb{R}$, $\alpha > 0$ $i \in \{1, 2, 3\}$ and x_i is the i^{th} coordinate of the vector \mathbf{x} , one finds that u is a solution to (3.32) if

$$c = \alpha = \frac{1}{m}. \quad (3.34)$$

Figure 3.1: Front propagation (3.33) with $m = \frac{1}{\alpha} = 3$

In (3.33), we use the notation a_+ for the positive part of a , that is, $a_+ = \frac{1}{2}(|a| + a)$. Let us check that (3.33) is solution under the condition (3.34). Indeed, in such a case, we have

$$u(\mathbf{x}, t) = \left(\frac{t}{m} - x_i \right)_+^{\frac{1}{m}}, \quad \frac{\partial u}{\partial t} = \frac{1}{m^2} \left(\frac{t}{m} - x_i \right)_+^{\frac{1}{m}-1}, \quad \nabla u = -\frac{1}{m} \left(\frac{t}{m} - x_i \right)_+^{\frac{1}{m}-1} e_i,$$

where e_i is the i^{th} vector of the canonical basis. Hence,

$$\operatorname{div}(u^m \nabla u) = \frac{1}{m} \operatorname{div} \left[\left(\frac{t}{m} - x_i \right)_+^{\frac{1}{m}} e_i \right] = \frac{1}{m^2} \left(\frac{t}{m} - x_i \right)_+^{\frac{1}{m}-1},$$

hence u is a solution to (3.32).

The solution (3.33) is referred to as "Marshak wave" in the literature [27, 112, 104]. It is more involved in general for an equation similar to (3.23) [27, 136, 113], but the same kind of behavior (that is, propagation of the front at finite velocity) is still present. Further, it gives an analytical solution in a very particular situation, which is a good test for numerical methods. Note finally that it may be generalized to more complicated situations [83].

3.2.4 Flux limitation

When using the diffusion approximation (3.15), we assume implicitly that the flux F_ν is given by (3.14). However, as pointed out in Subsection 3.1.2, it is clear from the definition (3.12) that the inequality

$$|F_\nu| \leq cE_\nu$$

must be satisfied. This is not ensured by (3.15). Hence, the notion of flux limitation has been introduced to circumvent this difficulty [105, 114, 87, 140, 88, 107, 74]. The idea is the following: instead of using formula (3.14) to define the flux, one uses a non linear function of ∇E_ν which satisfies the following:

$$\frac{F_\nu}{cE_\nu} = X(|R_\nu|)R_\nu, \quad R_\nu = \frac{1}{\sigma_a(\nu) + \kappa_{\text{Th}}} \frac{\nabla E_\nu}{E_\nu}, \quad (3.35)$$

where $X : \mathbb{R}^+ \rightarrow \mathbb{R}^+$ is a function satisfying $|X(r)| \leq 1/r$. Moreover, we want to recover the diffusion limit, which corresponds to $|R_\nu| \rightarrow 0$ (see (3.10)), and in which case we should have $X = X(0) = 1/3$, according to (3.14). Another nice property is to recover the free streaming limit. In such a case, we have $|R| \rightarrow \infty$, according to (3.9). Moreover, solving explicitly the free streaming equation (forgetting about boundary condition for a while) gives $I_\nu(\mathbf{x}, t, \Omega) = I_\nu^0(\mathbf{x} - c\Omega t)$, hence,

according to (3.12), $F_\nu = R_\nu/|R_\nu|$. Hence, in order to recover both asymptotic regimes, we are lead to impose

$$\begin{cases} X(r) \sim \frac{1}{r} & \text{as } r \rightarrow \infty, \\ X(r) \rightarrow \frac{1}{3} & \text{as } r \rightarrow 0. \end{cases} \quad (3.36)$$

The first line of (3.36) correspond to the free streaming limit (3.9), and the second one to the diffusion limit. In addition, the corresponding diffusion equation now reads

$$\frac{\partial E_\nu}{\partial t} - \operatorname{div}(cE_\nu X(|R_\nu|)R_\nu) + c\sigma_a(\nu)(E_\nu - B_\nu(T_e)) = 0, \quad (3.37)$$

where R_ν is defined by (3.35). Two commonly used limitors X are given by

$$X(r) = \frac{1}{3+r}, \quad \text{and} \quad X(r) = \min\left(\frac{1}{r}, \frac{1}{3}\right).$$

The first one is called harmonic limitor, while the second one is referred to as "sharp cut-off". Many other possibilities have been proposed in the literature. We refer to [105, 114, 87, 88] among others for details.

Let us finally point out that, under physical considerations, a similar limitation of the flux may be applied to electronic and ionic conduction terms, through the definition of χ_e and χ_i in (3.2) and (3.3), respectively. It is commonly admitted that one needs a nonlocal limitation in order to get physically relevant fluxes. The study of these limitors is beyond the scope of the present document, and we refer to [122, 95, 96] for corresponding details.

3.3 Numerical schemes

We now turn to numerical methods used to simulate the radiative transfer equation in the diffusion limit. In principle, one should study (3.15) coupled with (3.2) and (3.3). A natural choice is to split the resolution into first solving (at each time step) (3.15), and then use its result to solve (3.2)-(3.3). Therefore, in order to simplify the presentation, we are going to study the discretization of (3.15), in which we consider T_e as fixed. We thus recall it for the sake of completeness:

$$\frac{\partial E_\nu}{\partial t} - \operatorname{div}\left(\frac{c}{3(\sigma_a(\nu) + \kappa_{\text{Th}})}\nabla E_\nu\right) + c\sigma_a(\nu)\left(E_\nu - \frac{4\pi}{c}B_\nu(T_e)\right) = 0. \quad (3.38)$$

3.3.1 Multigroup approximation

The first variable in which we are going to discretize (3.38) is the frequency ν . For this purpose, we define a set $\nu_1 < \nu_2 < \dots < \nu_{N_g-1}$ of $N_g - 1$ frequencies, and consider the N_g corresponding groups defined by

$$G_k = [\nu_{k-1}, \nu_k], \quad 1 \leq k \leq N_g, \quad (3.39)$$

with the convention that $\nu_0 = 0$ and $\nu_{N_g} = \infty$. Defining E_k as the radiative energy in each group (i.e the integral of E_ν over G_k), and integrating (3.38) over the group k , we find

$$\frac{\partial E_k}{\partial t} - \operatorname{div}\left(\int_{\nu_{k-1}}^{\nu_k} \frac{c}{3(\sigma_a(\nu) + \kappa_{\text{Th}})}\nabla E_\nu d\nu\right) + c \int_{\nu_{k-1}}^{\nu_k} \sigma_a(\nu)E_\nu d\nu - 4\pi \int_{\nu_{k-1}}^{\nu_k} \sigma_a(\nu)B_\nu(T_e) d\nu = 0.$$

In order to simplify this equation, we are going to make the assumption that E_ν is not far from being equal to $B_\nu(T_e)$. Therefore, the equation becomes

$$\frac{\partial E_k}{\partial t} - \operatorname{div}\left(\frac{c}{3\sigma_k^R}\nabla E_k\right) + c\sigma_k^P(E_k - b_k a T_e^4) = 0, \quad (3.40)$$

where we have set

$$\frac{1}{\sigma_k^R} = \left(\int_{\nu_{k-1}}^{\nu_k} B'_\nu(T_e) d\nu \right)^{-1} \int_{\nu_{k-1}}^{\nu_k} \frac{B'_\nu(T_e)}{\sigma_a(\nu, T_e) + \kappa_{\text{Th}}} d\nu, \quad (3.41)$$

$$\sigma_k^P = \left(\int_{\nu_{k-1}}^{\nu_k} B_\nu(T_e) d\nu \right)^{-1} \int_{\nu_{k-1}}^{\nu_k} \sigma_a(\nu, T_e) B_\nu(T_e) d\nu, \quad (3.42)$$

and

$$b_k = \frac{\int_{\nu_{k-1}}^{\nu_k} B_\nu(T_e) d\nu}{\frac{acT_e^4}{4\pi}} = \frac{\int_{\nu_{k-1}}^{\nu_k} B_\nu(T_e) d\nu}{\int_0^\infty B_\nu(T_e) d\nu}. \quad (3.43)$$

Of course, the choice of the coefficients in (3.40) is not obvious. Actually, it relies on the strong hypothesis that (as far as these coefficients are concerned) $E_\nu \approx B_\nu(T_e)$. However, if the sizes of the groups are sufficiently small, then such an assumption almost does not change the values of the coefficients. Further, these values ensure that the equilibrium is respected, namely that if $E_k = \frac{acT_e^4}{4\pi} b_k$, then $\partial_t E_k = 0$.

3.3.2 Time and space discretization

Time discretization

For the time discretization, since all equations we have to solve contain diffusion terms, a natural choice is to use an implicit or semi-implicit discretization. Then the resolution of the coupled system is splitted into first solving (3.40) implicitly, that is

$$\frac{E_k^{n+1} - E_k^n}{\Delta t} - \text{div} \left(\frac{c}{3\sigma_k^R} \nabla E_k^{n+1} \right) + c\sigma_k^P (E_k^{n+1} - b_k a(T_e^n)^4) = 0, \quad (3.44)$$

where all the coefficients are computed in an explicit way, that is, using the variables at time step n . Here, Δt is the time step. Then, one solves the ionic and electronic equations, for which an implicit scheme is used.

Space discretization

Considering (3.44), we are thus lead to discretize it in the space variable. Here, it is important to recall that the system is coupled to hydrodynamics. The corresponding scheme uses piecewise constant thermodynamic variables. Hence, finite volume methods are a natural choice for this.

Let us also recall that the preferred choice for the hydrodynamics is a lagrangian scheme. Hence, the mesh may be highly deformed by the flow, especially if hydrodynamics instabilities are present. An example of such a mesh is given in Figure 3.2. Starting from a regular mesh, we end with a highly deformed one, some of the cells having very poor aspect ratio. Thus, the question is:

Define a finite volume scheme for piecewise constant unknown of an elliptic equation on deformed meshes.

In order to make precise this question, let us define a model problem: we want to solve the equation

$$-\text{div}(D\nabla u) = f \quad \text{in } \mathcal{D}, \quad (3.45)$$

with adapted boundary conditions (say, Dirichlet boundary conditions $u|_{\partial\mathcal{D}} = u^{\text{ext}}$.) We thus want to solve this problem with a piecewise constant unknown u and data f and D on a deformed, possibly unstructured, mesh. The properties we want the scheme to satisfy are the following:

1. the scheme should be convergent, hopefully of order 2;
2. the scheme should be stable;

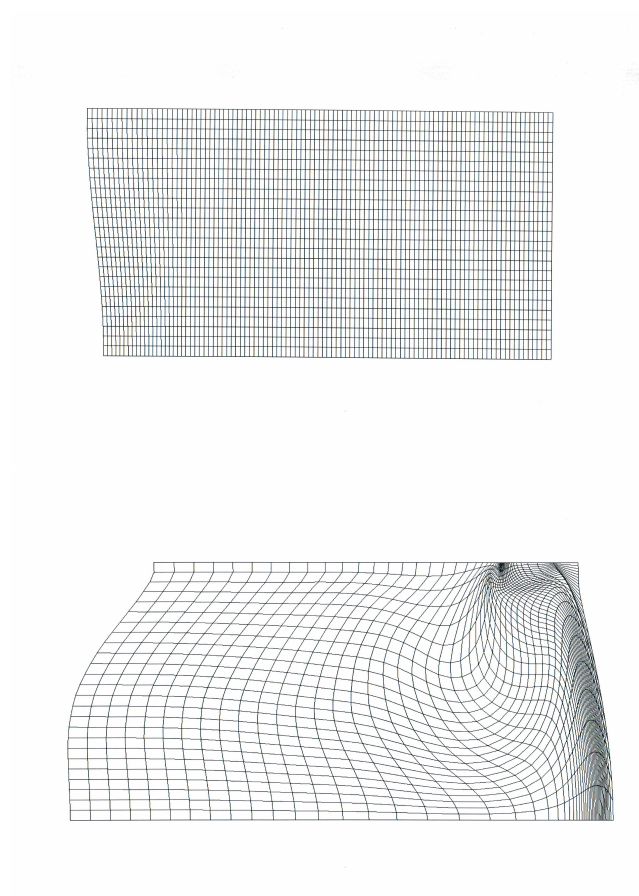


Figure 3.2: An example of mesh produced by a lagrangian simulation in the case of development of instability: beginning of simulation (left) and end of simulation (right)

3. the scheme should satisfy the (discrete) maximum principle;
4. the scheme should be linear;
5. the matrix produced by the scheme should be symmetric;
6. one should recover the five point scheme (see below) on an orthogonal mesh.

These properties are more or less given from the most important to the less important. However, this order is highly subjective and may be thought of differently. For instance, one may think that convergence at order two may (or may not) be dropped in favor of satisfying the maximum principle.

We are first going to study the most simple scheme, that is, the five-point scheme, and show why it fail to satisfy item 1 (although it does satisfy items 2 to 5). Then we will very briefly review some scheme proposed in the literature, and focus in particular on a very natural and simple one which satisfies all the above properties except that it is convergent only at order one.

Before going on with the presentation of these schemes, we give some notation. We stick to the two-dimensional case, for the sake of simplicity, and assume quadrangular meshes. However, all the following is also valid for general polyhedron meshes. The mesh will be denoted by \mathcal{T} , and is a set of cells, generically denoted by K . This mesh covers the simulation domain \mathcal{D} :

$$\overline{\mathcal{D}} = \overline{\bigcup_{K \in \mathcal{T}} K}.$$

The boundary between a cell K and one of its neighbouring cells L will be denoted by $K|L$:

$$K|L = \overline{K} \cap \overline{L}.$$

We define $n_{K|L}$ as the unit vector which is orthogonal to $K|L$ towards L . Hence, $n_{K|L} = -n_{L|K}$. For each $K \in \mathcal{T}$, we denote by $\mathbf{x}_K \in K$ the "center" of K . This can be the center of mass of the cell K , or some different point, depending on the scheme we define. In the following, we always assume that \mathbf{x}_K is the center of mass of K . Of course, we do not assume that for two neighbouring cells K and L , the segment $[\mathbf{x}_K, \mathbf{x}_L]$ is orthogonal to $K|L$. This property ensures the diffusion finite volume scheme to have good properties (see [49] and the references therein), but the meshes we consider here are not sufficiently regular for this property to hold.

Five-point scheme The starting point of all finite volume schemes is to integrate (3.45) over a cell K and use Green's formula:

$$\int_{\partial K} D \nabla u \cdot \mathbf{n} = - \int_K f. \quad (3.46)$$

Hence, the main question is, using an approximation of u which is constant on each cell, how can we compute an approximation of its gradient, or more precisely an approximation of its flux across the boundary of a cell K (left-hand side of (3.46)). Let us assume for a while that $D = 1$, which allows to write

$$\int_{\partial K} \frac{\partial u}{\partial n} = - \int_K f. \quad (3.47)$$

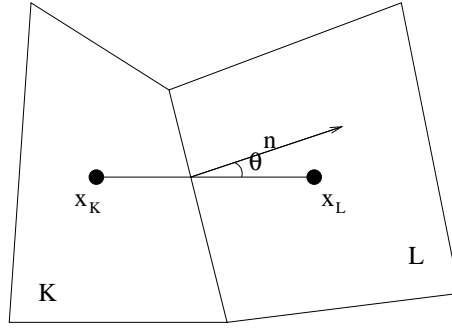
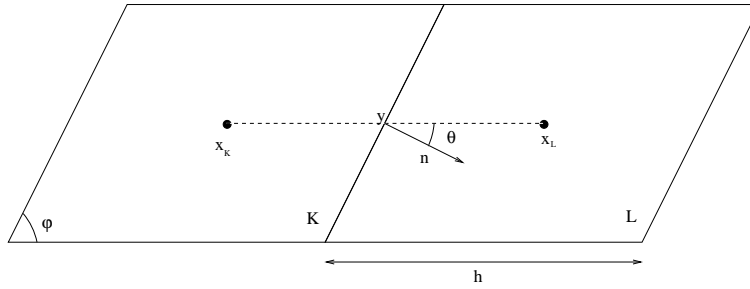
A natural choice to approximate the flux is to use a Taylor approximation of the gradient on the boundary between two cells. Hence, considering two cells K and L , we write

$$\forall \mathbf{x} \in K|L, \quad \nabla u(\mathbf{x}) \approx \frac{u(\mathbf{x}_L) - u(\mathbf{x}_K)}{|\mathbf{x}_L - \mathbf{x}_K|} \frac{\mathbf{x}_L - \mathbf{x}_K}{|\mathbf{x}_L - \mathbf{x}_K|},$$

hence

$$\frac{\partial u}{\partial n_{K|L}} \approx \frac{u(\mathbf{x}_L) - u(\mathbf{x}_K)}{|\mathbf{x}_L - \mathbf{x}_K|} \frac{\mathbf{x}_L - \mathbf{x}_K}{|\mathbf{x}_L - \mathbf{x}_K|} \cdot \mathbf{n}_{K|L} = \frac{u(\mathbf{x}_L) - u(\mathbf{x}_K)}{|\mathbf{x}_L - \mathbf{x}_K|} \cos(\theta_{K|L}), \quad (3.48)$$

where $\theta_{K|L}$ is the angle between $\mathbf{n}_{K|L}$ and the segment $[\mathbf{x}_K, \mathbf{x}_L]$ (see figure 3.3). Hence, setting

Figure 3.3: Taylor approximation of the flux accross $K|L$.Figure 3.4: Cells K and L with the corresponding vector $\mathbf{n}_{K|L}$

$u_K = u(\mathbf{x}_K)$ and $f_K = f(\mathbf{x}_K)$, one ends up with the formula, valid for any $K \in \mathcal{T}$:

$$|K|f_K = \sum_{L \in \mathcal{N}(K)} \ell(K|L) \frac{u_K - u_L}{|\mathbf{x}_K - \mathbf{x}_L|} \cos(\theta_{K|L}), \quad (3.49)$$

where $\mathcal{N}(K)$ denotes the set of neighbouring cells of K , $\theta_{K|L}$ is the angle between the $[\mathbf{x}_K, \mathbf{x}_L]$ and $\mathbf{n}_{K|L}$, and $\ell(K|L)$ is the length of the edge which is shared by K and L . Note that the matrix corresponding to the system (3.49) is an M-matrix. Hence, this scheme satisfies a discrete version of the maximum principle. However, we will show that it is not consistent. Indeed, consider two neighbouring cells K, L as in figure 3.4: \mathbf{y} is the middle point of $K|L$, and $\theta = \theta_{K|L} = \frac{\pi}{2} - \varphi$. Hence, computing the approximation of the flux (3.48), we have, using a Taylor expansion around \mathbf{y} ,

$$\frac{u(\mathbf{x}_L) - u(\mathbf{x}_K)}{|\mathbf{x}_L - \mathbf{x}_K|} \cos(\theta_{K|L}) = \frac{\partial u}{\partial x_1}(\mathbf{y}) \sin(\varphi) + O(h).$$

We can also compute explicitly:

$$\nabla u(\mathbf{y}) \cdot \mathbf{n} = \frac{\partial u}{\partial x_1}(\mathbf{y}) \sin(\varphi) - \frac{\partial u}{\partial x_2}(\mathbf{y}) \cos(\varphi).$$

Hence, we see that, as far as $\varphi \neq \frac{\pi}{2}$, the approximation (3.48) cannot be consistent. This is corroborated by simple numerical experiments.

Some other schemes The fact that the five-point scheme is not convergent on deformed meshes has been known for a long time. Therefore, the definition of a scheme adapted to such a situation has been a very active field of research for some thirty years. Let us give now a (very brief) overview of the methods which have been proposed to date.

- One of the first finite volume scheme in the framework of arbitrary mesh is the Kershaw scheme, presented in [75]. Roughly speaking, it consists in using additional neighbouring cells to compute the approximate flux. This scheme is of order 2, produces a symmetric matrix,¹ but does not satisfy the maximum principle.

¹if D is symmetric

- In the same vein, the diamond scheme was proposed in [32]: the gradient in the tangential direction is approximated using the values of the unknown at the nodes. For each node, the value of the unknown is computed using an interpolation on the cells containing this node. This scheme is not widely used since it produces a non-symmetric matrix, which in some situations is badly conditioned.
- Another approach is to use a mixed finite element method to solve the diffusion equation. By doing so, one introduces additional degrees of freedom, namely the value of the unknown on the faces of the cells. Then, using a hybrid formulation, one eliminates the cell-centered values and solves the system giving these new degrees of freedom. An example of such a scheme is described in [5]. This scheme is of order 2, produces a symmetric matrix,² but does not satisfy the maximum principle.
- More recently, the discrete duality finite volume method (DDFV) was proposed in [67, 63, 64, 65, 66]. Here again, one introduces additional degrees of freedom to improve the approximation of the gradient. These additional degrees of freedom are defined on a dual mesh. The global system (original and additional unknowns) is then solved as whole. This scheme is of order 2, produces a non-symmetric matrix, and does not satisfy the maximum principle.
- Another method is called the Mimetic Finite Difference [20, 19, 93], and is based on imitating the properties of the original continuum differential operators such as, for instance, Green formula. Here, the flux of each face is introduced as an unknown, and the global system (centered values and fluxes) is solved. Such a scheme is convergent of order 2, produces a symmetric matrix,² but does not satisfy the maximum principle.
- The scheme using stabilization and harmonic interfaces (SUSHI) method [48] is based on an idea similar to the diamond scheme. However, a "stabilization" term is added to the discrete gradient, which improves the consistency. It is convergent of order 2, produces a symmetric matrix,² and does not satisfy the maximum principle.
- The multipoint flux approximation (MPFA), proposed by [15, 1], also introduces additional degrees of freedom on the boundary of the cells, but possibly at several points at each face. These additional degrees of freedom are used to compute more precisely the numerical flux, and then are eliminated by imposing the continuity of the flux on each face. These schemes are convergent of order 2 (except on random meshes), produce non-symmetric matrices, and do not satisfy the maximum principle.
- In [40], a similar strategy was used to derive a *nonlinear* scheme, which is convergent at order 2 and satisfies the maximum principle.
- The finite difference scheme of [85] aims at using consistent (for the second derivative) formulas, by allowing a larger stencil. This scheme produces a symmetric matrix,² is convergent of order 1, and satisfies the maximum principle.
- The "Laplacian Integration" (LapIn) scheme, proposed in [134], uses the Voronoï mesh in order to recover orthogonal properties. A kind of five-point finite volume scheme is then used on this secondary mesh. The scheme is convergent at order 1, produces a symmetric matrix,² and satisfies the maximum principle.

Let us conclude by indicating that the above list is by no means exhaustive. Moreover, some of these methods show very similar behaviour, and may become equivalent in some situations. See [143] for details. Finally, we point out that a similar review was given in [14].

LapIn scheme We are now going to explain in details the method LapIn (Laplacian Integration), proposed in [134, 133]. The idea is to use a secondary mesh instead of the one imposed by the hydrodynamics scheme. The main advantage of this scheme is that it satisfies the maximum principle, while being linear. However, this comes at the price of letting down convergence at order

²if D is symmetric

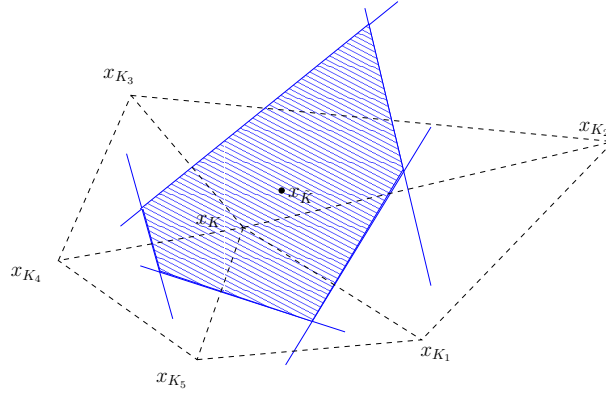
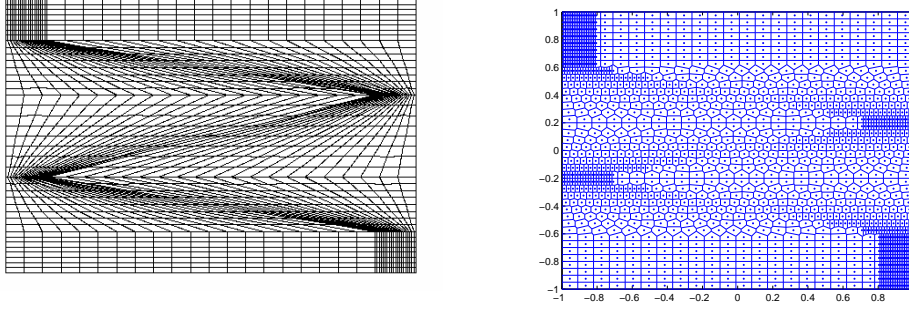
Figure 3.5: Construction of the Voronoi cell around a point \mathbf{x}_K 

Figure 3.6: Example of a distorted mesh (left) and the corresponding Voronoi mesh (right)

2. Here again, we use the above notation, namely \mathcal{T} is the mesh (the set of cells), $K|L = \bar{K} \cap \bar{L}$ is the common boundary of cells K and L , and \mathbf{x}_K is the center of mass of K . We will detail the scheme only with homogeneous Neumann boundary conditions, in order to avoid technicalities. It is however possible to include different boundary conditions.

To the set of points $\{\mathbf{x}_K, K \in \mathcal{T}\}$, we associate its Voronoi mesh. This mesh is defined as follows:

$$\forall K \in \mathcal{T}, \quad \tilde{K} = \{\mathbf{x} \in \mathcal{D}, \forall L \neq K, |\mathbf{x} - \mathbf{x}_K| \leq |\mathbf{x} - \mathbf{x}_L|\}. \quad (3.50)$$

This is explained in figure 3.5 In other words, the new cell \tilde{K} is the set of points which closer to \mathbf{x}_K than to any other center of mass. See figure 3.6 for an example of such a mesh.

We then write down a finite volume scheme on the new mesh. The advantage is that any segment $[\mathbf{x}_{\tilde{K}}, \mathbf{x}_{\tilde{L}}]$ of two neighbouring (in the Voronoi mesh) cell centers is orthogonal to the corresponding face. Hence, the approximation of the flux by the five-point scheme becomes consistent.

Let us first focus on the case of the Laplace operator (i.e the diffusion coefficient is constant). Then, we use the standard finite volume approach to write:

$$\begin{aligned} |\tilde{K}|f(\mathbf{x}_{\tilde{K}}) &\approx \int_{\tilde{K}} -\Delta u = \int_{\partial\tilde{K}} \frac{\partial u}{\partial n} \\ &= - \sum_{\tilde{L} \in \mathcal{N}(\tilde{K})} \int_{\tilde{K}|\tilde{L}} \frac{\partial u}{\partial n} \approx \sum_{\tilde{L} \in \mathcal{N}(\tilde{K})} \ell(\tilde{K}|\tilde{L}) \frac{u(\mathbf{x}_K) - u(\mathbf{x}_L)}{|\mathbf{x}_K - \mathbf{x}_L|}. \end{aligned}$$

Assuming that $f(\mathbf{x}_{\tilde{K}}) \approx f(\mathbf{x}_K)$, we thus have a finite volume scheme for Laplace's operator.

Now, if the coefficient diffusion is not constant, assuming that it is sufficiently smooth, we write:

$$\begin{aligned} -\operatorname{div}(D\nabla u) &= -D\Delta u - \nabla d \cdot \nabla u = -\frac{1}{2}\left(D\Delta u + \Delta(Du)\right) - \frac{1}{2}\left(\nabla D \cdot \nabla u - \operatorname{div}(u\nabla D)\right) \\ &= -\frac{1}{2}\left(D\Delta u + \Delta(Du)\right) + \frac{1}{2}u\Delta D. \end{aligned}$$

Hence, up to the addition of a diagonal operator, the operator $-\operatorname{div}(D\cdot)$ is equal to the symmetric part of the operator $-D\Delta$. Hence, having computed the Laplace operator on the Voronoï mesh, one easily computes $-\operatorname{div}(D\cdot)$ by multiplying the previous one by D , then taking its symmetric part, and finally adding up a diagonal operator.

Finally, the scheme may be summarized as follows:

1. compute the Voronoï mesh $\tilde{\mathcal{T}}$;
2. compute the matrix corresponding the discretization of $-\Delta$ on $\tilde{\mathcal{T}}$, which we call $M_{\tilde{\mathcal{T}}}(-\Delta)$;
3. multiply each line of $M_{\tilde{\mathcal{T}}}(-\Delta)$ by the corresponding coefficient $D(\mathbf{x}_K)|K|/|\tilde{K}|$;
4. symmetrize the matrix;
5. add up on the diagonal a term so that the sum of each line is zero.

By doing so, we have explicitly constructed an M -matrix, so the maximum principle of this scheme is respected. Moreover, should the original mesh be a Voronoï mesh, then the scheme would reduce to classical finite volume schemes [137, 106, 49], which are known to be convergent at order two. However, if this is not the case, since we have assumed that

$$f(\mathbf{x}_K) \approx f(x_{\tilde{K}}),$$

in the above scheme, and since this equality is valid up to an error of order h (the size of the mesh), we end up with an order one scheme on general meshes.

This scheme has been tested on simple cases, and numerical study of convergence indicates an order between 1 and 2, depending whether the center of mass of cells K are close to those of the Voronoï cells or not. We refer to [134, 133] for other details on this scheme.

As an example, let us consider the following test case, borrowed from [134]:

$$\begin{cases} -\Delta u + \omega^2 u = \omega^2 \mathbf{1}_{x_1 \leq 0} & \text{in } \mathcal{D} = (-1, 1)^2, \\ \partial_n u = 0 & \text{on } \partial\mathcal{D}, \end{cases} \quad (3.51)$$

with $\omega = 1$. The solution of this problem is explicit, and depends only on x_1 :

$$u(\mathbf{x}) = \begin{cases} 1 - \frac{\cosh(\omega(x_1+1))}{2 \cosh(\omega)}, & \text{if } x_1 < 0, \\ \frac{\cosh(\omega(x_1-1))}{2 \cosh(\omega)} & \text{if } x_1 > 0. \end{cases}$$

Figure 3.7 gives the result of the five-point scheme (in blue) and of the DDFV scheme [65] (in red), when using a Kershaw-type mesh (figure 3.6 left). The first does not have any overshoot (or undershoot), but is inaccurate. The second one is accurate, but has overshoots and undershoots. On the contrary, as shown in figure 3.8, the LapIn scheme is more accurate than the five-point scheme, and satisfies the maximum principle.

3.4 Higher order models

Going back to the radiative transfer equation, since the materials in the capsule are almost transparent (at least at the beginning of the simulation), one should note that the diffusion approximation is questionable. Nevertheless, flux limiters allow to extend the validity of this approximation to this case. However, a natural question is: can we find a different way carry out such a computation?

The first possibility is to solve directly the radiative transfer equation. For this, mainly two methods are available:

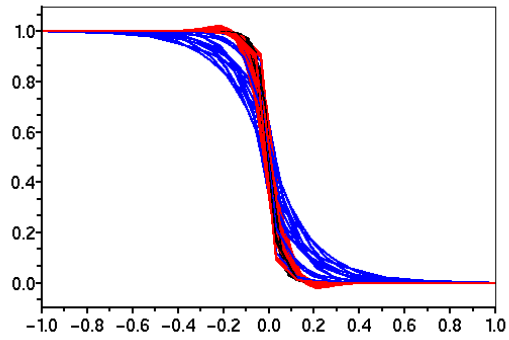


Figure 3.7: Test case (3.51) with Kershaw mesh. Five-point scheme (blue), and DDFV (red)

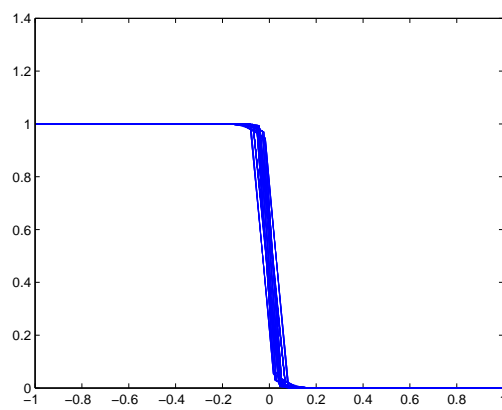


Figure 3.8: Test case (3.51) with Kershaw mesh. LapIn scheme

- Monte Carlo methods: these are not adapted to implosion simulations, because they are very sensitive to hydrodynamical instabilities. Thus, statistical noise prevents any reliable computation.
- Discrete ordinate methods. These methods consists in discretizing the angular variable, using a piecewise constant approximation [108, 9, 45, 90, 104]. However, such methods are very expensive, hence cannot be used in realistic computations.

Beside these two possibilities, another approach is to use an approach similar to the one described in Subsection 3.1.2. Indeed, instead of assuming a P1 approximation for the radiative intensity, one can use a polynomial expansion of higher degree. In order to simplify the presentation, we restrict ourselves to the one-dimensional case, although the generalization to higher dimensions is not a problem. In this case, we replace the angular variable $\Omega \in S^2$ by $\mu \in [-1, 1]$, which is the azimuthal angle [28]. Hence, (3.1) becomes

$$\frac{1}{c} \frac{\partial I_\nu}{\partial t} + \mu \frac{\partial I_\nu}{\partial x} + \sigma_a(\nu) (I_\nu - B_\nu(T_e)) + \kappa_{\text{Th}} \left(I_\nu - \frac{1}{2} \int_{-1}^1 I_\nu(\mu') d\mu' \right) = 0. \quad (3.52)$$

We assume a development of I_ν on the basis of Legendre polynomials:

$$I_\nu(x, t, \mu) = \sum_{n \geq 0} J_n(x, t, \nu) P_n(\mu). \quad (3.53)$$

Using the induction relation of the Legendre polynomials, we find

$$\begin{aligned} \frac{1}{c} \frac{\partial J_n}{\partial t} + \frac{\partial}{\partial x} \left(\frac{n+1}{2n+1} J_{n+1} - \frac{n}{2n+1} J_{n-1} \right) + (\sigma_a(\nu) + \kappa_{\text{Th}}) J_n \\ = \sigma_a(\nu) B_\nu(T_e) \delta_{n0} + \kappa_{\text{Th}} \delta_{n0} J_0, \end{aligned}$$

with the convention that $J_{-1} = J_{N+1} = 0$. This may be seen as a hierarchy of coupled equations. This is called the PN approximation [81, 82], since (3.53) corresponds to assuming that I_ν is a polynomial of degree N with respect to μ . Note that in the case $N = 1$, we recover the system (3.13). For N larger than 1, the system is a more precise approximation of (3.1). It is however more difficult to solve, since it contains $(d^{n+1} - 1)/(d - 1)$ unknowns, where d is the dimension (this value is $N + 1$ if $d = 1$). Moreover, it assumes that I_ν is a smooth function of Ω (or μ in dimension one), and therefore is a poor approximation in the free streaming limit. Indeed, in this limit, I_ν is a Dirac mass as a function of Ω .

Another possibility is to use the discrete ordinate method, which assumes that I_ν is a piecewise constant function of Ω . See for instance [108] and the references therein. Finally, let us also mention a different closure method, called the M1 method, which consists in writing down the two first moments of equation (3.1), which involve E_ν , F_ν (as defined by (3.12)), and the second moment

$$P_\nu = \frac{1}{c} \int_{S^2} \Omega \otimes \Omega I_\nu(\Omega) d\Omega,$$

which is called the radiative pressure tensor:

$$\begin{cases} \frac{\partial E_\nu}{\partial t} + \text{div}(F_\nu) + c\sigma_a(\nu) \left(E_\nu - \frac{4\pi}{c} B_\nu(T_e) \right) = 0, \\ \frac{1}{c} \frac{\partial F_\nu}{\partial t} + c \text{div}(P_\nu) + (\sigma_a(\nu) + \kappa_{\text{Th}}) F_\nu = 0. \end{cases} \quad (3.54)$$

In order to close this system, we need to express P_ν as a function of F_ν and E_ν . The P1 approximation correspond to $P_\nu = \frac{1}{3} E_\nu$, but many other closures are possible. Such a closure is usually based on entropy minimization [41, 89, 62, 33, 108, 141].

Note that if one solves these kind of hyperbolic systems (that is, PN or M1) using an explicit scheme, then, as is apparent in the second line of (3.54), the CFL condition involves the speed of light c , and is therefore very restrictive. Hence, it is mandatory to use an implicit scheme.

Moreover, important issue is to use a numerical scheme which recovers the diffusion limit. This is called an "asymptotic preserving" scheme. It is *a priori* not obvious for a given hyperbolic scheme to satisfy such a property. We refer to [22, 60, 73, 58, 59, 2] for details on this issue.

Chapter 4

Hele-Shaw models

4.1 Introduction

The material presented below has been developed in collaboration with H. Egly and R. Sentis.

An ablation front is where a steep temperature gradient enters in a hydrodynamic zone. The consequence is a very strong rocket effect, which is in fact favorable for the compression of the thermonuclear fuel in ICF experiments [92]. It has been observed, Takabe et al. [138], that the ablation phenomena stabilized long wavelength linear instabilities. Further theoretical and numerical studies enlighten the ablation Rayleigh-Taylor instabilities in linear regime, see for example [101]. An important difficulty is to model ablation fronts. For the the simulation of ablation instabilities in the non linear regime, one must account for compressible Euler model with thermal conduction. Direct Numerical Simulation of this kind of problem is very heavy and tricky, indeed it leads to deal with wavelengths at different scales; moreover one addresses low Mach number flows, then explicit numerical schemes for the hydrodynamics part would be stable only with a strong constraint on the time step therefore it would be necessary to perform a lot of time steps and there is a risk that numerical diffusion would be as important as the physical diffusion. In some situations, shortly described in the following, it is possible to model ablation fronts with a simplified Hele-Shaw type model [46, 47]. According to the works of J. Sanz and others [111, 119, 120, 4], the idea is to model the evolution of the temperature (to power n) with a Poisson equation solved on a domain corresponding to the hot region and a zero Dirichlet boundary condition on a moving ablation front. Afterwards the coupling with hydrodynamics flow is insured via a Bernoulli like equation.

The starting point is the compressible Euler model

$$\begin{cases} \partial_t \rho + \nabla \cdot (\rho \mathbf{u}) = 0 \\ \partial_t \rho \mathbf{u} + \nabla \cdot (\rho \mathbf{u} \otimes \mathbf{u}) + \nabla p = 0 \\ \partial_t (\rho e) + \nabla \cdot (\rho \mathbf{u} e + p \mathbf{u}) - \nabla \cdot (\kappa n T^n \nabla T) = 0 \end{cases} \quad (4.1)$$

written in the domain Ω described in figure 4.1 corresponding to a spherical shell. The total energy e is given by $e = \mathcal{E} + \frac{1}{2}|\mathbf{u}|^2$ where \mathcal{E} is the internal energy; T denotes the temperature and $p = (\gamma - 1)\rho\mathcal{E} = \rho T$ the pressure; so $\mathcal{E} = C_v T$. The two first equations are related to the evolution of the density ρ and the velocity \mathbf{u} , the third one is the total energy balance with a non linear heat flux, it reads also

$$\partial_t (\rho \mathcal{E}) + \nabla \cdot (\rho \mathbf{u} \mathcal{E}) + p \nabla \cdot \mathbf{u} - \nabla \cdot (\kappa n T^n \nabla T) = 0$$

The energy equation has to be supplemented by a boundary condition on the external boundary Γ_e which is a non-homogeneous Neumann condition (related to the heating of the spherical shell by a thermal flux) and by a Dirichlet condition on the inner boundary Γ_c . On the external boundary Γ_e , since the velocity is outwards, there is no boundary condition for the equations of the density and of momentum.

We make some remarks which are at the basis of the modeling.

- In the experiments we have in mind, the material is initially cold and dense and is ablated by the thermal flux at a surface denoted by $\Gamma_f(t)$ called "ablation front"; this surface is moving

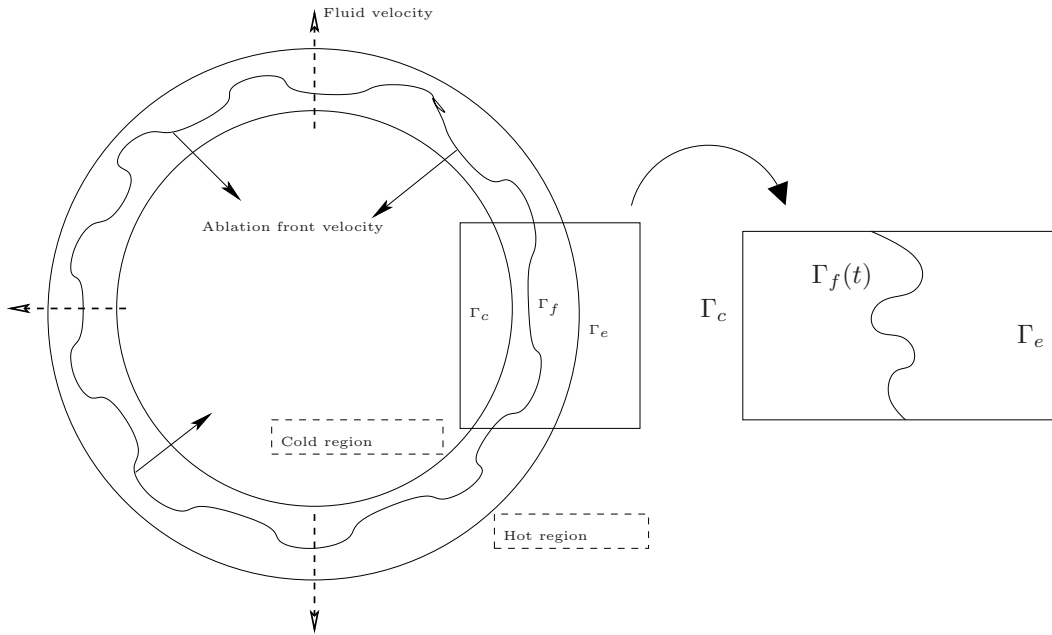


Figure 4.1: ICF convergent geometry. A heat flux comes from the external boundary Γ_e , so that an ablation front Γ_f propagates towards the center of the shell. The front Γ_f may be considered as a moving frontier. Notice the equivalence with Cartesian geometry.

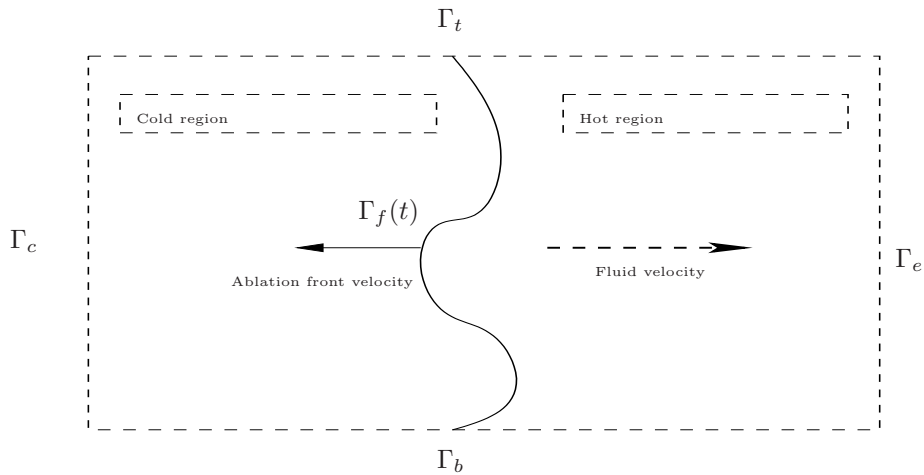


Figure 4.2: A zoom near the ablation front Γ_f which propagates towards the left of the domain.

and propagates inwards. In the neighborhood of Γ_f the density varies with a sharp gradient from the cold region where $\rho \simeq \rho_c$ (with ρ_c constant) to the hot region where $\rho \ll \rho_c$; and there the temperature varies from $T \simeq T_c$ to the hot level $T \gg T_c$. This is represented in figure 4.3 which is a cut along the radial direction. The subscript ${}_c$ refers to the cold region.

- As shown in figure 4.1, it may be assumed that the geometry is locally planar, at least for the sake of simplicity to perform the following change of referential. One must account for the fact that a first shock have traveled through the ablative matter and a reflective shock travels from the inner boundary Γ_c towards the external one. Then the ablative matter is driven with a macroscopic velocity $\mathbf{u}_{\text{macro}}$; this velocity has a direction normal the boundaries Γ_c , is oriented inwards and its modulus is a given function which is assumed to depend smoothly on the time variable. We will

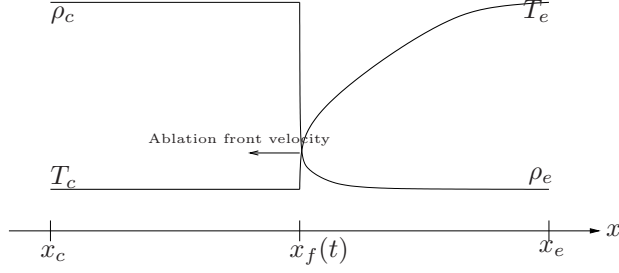


Figure 4.3: Radial cut, shape of density and thermal fields. The velocity of the front is $\dot{\Gamma}_f(t) < 0$

now state the system in the referential which moves with this velocity and we define x' by

$$x' = x - \int_0^t \mathbf{u}_{\text{macro}}(\tau) d\tau.$$

Now denoting by the primes (\cdot') the quantities evaluated in the moving referential

$$\mathbf{u}'(t, x') = \mathbf{u}(t, x) - \mathbf{u}_{\text{macro}}, \quad \rho'(t, x') = \rho(t, x), \quad T'(t, x') = T(t, x).$$

One gets after elementary manipulations

$$\begin{cases} \partial_t \rho' + \nabla' \cdot (\rho' \mathbf{u}') = 0 \\ \partial_t \rho' \mathbf{u}' + \nabla' \cdot (\rho' \mathbf{u}' \otimes \mathbf{u}') + \nabla' p' = \rho' \mathbf{g} \\ \partial_t (\rho' \mathcal{E}') + \nabla' \cdot (\rho' \mathbf{u}' \mathcal{E}') + p' \nabla' \cdot \mathbf{u}' - \nabla' \cdot (\kappa n T'^m \nabla T') = 0 \end{cases} \quad (4.2)$$

where we have introduced the acceleration $\mathbf{g} = \frac{\partial}{\partial t} \mathbf{u}_{\text{macro}}$.

4.2 The quasi-isobar model

On the schematic representation of figure 4.3, the ablative front is a singular surface where both the density and the temperature have very strong gradients; figure 4.3 is a cut of the map of these quantities along the radial direction. But we may assume that the pressure which is proportional to the product of the density and the temperature has a much smaller gradient, then it is approximately constant across the ablation front. This fact corresponds to the quasi-isobar assumption which is related to the low Mach number approximation; we address this approximation now.

Using the Lagrangian derivative and dropping the primes, system (4.2) reads as

$$\begin{cases} (\partial_t + \mathbf{u} \cdot \nabla) \rho + \rho \nabla \cdot \mathbf{u} = 0 \\ \rho (\partial_t + \mathbf{u} \cdot \nabla) \mathbf{u} + \nabla p = \rho \mathbf{g} \\ \frac{1}{\gamma - 1} (\partial_t + \mathbf{u} \cdot \nabla) p + \frac{\gamma}{\gamma - 1} p \nabla \cdot \mathbf{u} - \nabla \cdot (\kappa n T^n \nabla T) = 0. \end{cases} \quad (4.3)$$

Heuristically, the low Mach number approximation may be viewed as follows; see the appendix for a quick justification, see also [3] or [61] for a more rigorous analysis. First we assume that the pressure $p = \rho T$ is roughly constant that is to say, after a good scaling we set

$$\rho T = 1.$$

Secondly we introduce the variation of pressure P : the system to be solved reads as

$$\begin{cases} (\partial_t + \mathbf{u} \cdot \nabla) \rho + \rho \nabla \cdot \mathbf{u} = 0 \\ \rho (\partial_t + \mathbf{u} \cdot \nabla) \mathbf{u} + \nabla P = \rho \mathbf{g} \\ \nabla \cdot (\mathbf{u} - n T^n \nabla T) = 0. \end{cases} \quad (4.4)$$

The last equation means that the velocity is the sum of a thermal velocity and a vortex velocity which is divergence-free, that is to say $\mathbf{u} = \mathbf{u}_{\text{therm}} + \mathbf{u}_{\text{vort}}$, with

$$\mathbf{u}_{\text{therm}} = n T^n \nabla T \quad \text{and} \quad \nabla \cdot \mathbf{u}_{\text{vort}} = 0. \quad (4.5)$$

The density equation may be recast as

$$\partial_t \frac{1}{T} + \nabla \cdot \left(\frac{1}{T} n T^n \nabla T \right) + \nabla \cdot \left(\frac{1}{T} \mathbf{u}_{\text{vort}} \right) = 0$$

Therefore, multiplying the impulse equation by T and using the notation $\theta = T^n$ and $\nu = 1/n$, this model reads as

$$\begin{cases} \partial_t \theta^{-\nu} + \mathbf{u}_{\text{vort}} \cdot \nabla \theta^{-\nu} + \Delta \theta = 0, \\ \partial_t \mathbf{u} + \mathbf{u} \cdot \nabla \mathbf{u} + \theta^\nu \nabla P = \mathbf{g}, \\ \mathbf{u} = \theta^\nu \nabla \theta + \mathbf{u}_{\text{vort}}, \\ \nabla \cdot \mathbf{u}_{\text{vort}} = 0. \end{cases} \quad (4.6)$$

The sources of this system are the acceleration \mathbf{g} and the thermal flux at the external boundary. The system has four independent unknowns θ , \mathbf{u} , P and \mathbf{u}_{vort} . The pressure P may be understood as the Lagrange multiplier associated to the free divergence constraint $\nabla \cdot \mathbf{u}_{\text{vort}} = 0$. In the sequel we denote θ_{ref} a characteristic value of the temperature (to n -th power) in the external part of the simulation domain. Lastly, notice that the ablation phenomena is very sensitive to small perturbations, that is to say the ablation front propagation is unstable in nature. This is why we need to carefully describe the initial conditions. At $t = 0$, in the cold region, one assumes that $\rho \approx \rho_c$ is almost constant and the temperature also $\theta \approx \theta_c$. Moreover, we have

$$\theta_c / \theta_{\text{ref}} = \varepsilon \ll 1 \quad (4.7)$$

The vortex velocity \mathbf{u}_{vort} can be considered as small in a first step. Thus, in the following section we withdraw this term. Then the equation for the temperature reduces to $\partial_t \theta^{-\nu} + \Delta \theta = 0$. Convenient boundary conditions must be imposed on both parts Γ_c and Γ_e of the simulation domain; the normal external thermal flux is a data b^0 which depends slowly on time. So we have to address the equation

$$\begin{cases} \frac{\partial}{\partial t} (\theta^{-\nu}) + \Delta \theta = 0, \\ \theta = \theta_c, \\ \partial_n \theta = b^0, \end{cases} \quad \begin{array}{l} x \in \Gamma_c, \\ x \in \Gamma_e. \end{array} \quad (4.8)$$

As usual, $\partial_n = \partial / \partial n$ denotes the normal derivative.

4.3 Hele-Shaw models

The idea is to model the temperature field $\Theta \geq 0$ in a moving domain, so that $\Theta = 0$ is the equation of the ablation front. It can be proved that, in a quasi-incompressible regime relevant if the gas is modeled by a perfect gas equation of state and the structure of the ablation front is the one displayed in figure 1.4, the following Hele-Shaw model is relevant

$$\begin{cases} -\Delta \Theta = 0, & x \in \Omega_{\text{hot}}, \\ \partial_n \Theta = v, & x \in \Gamma_e, \\ \Theta = 0, & x \in \Gamma_f, \end{cases} \quad (4.9)$$

$$\dot{x}(t) = -\nabla \Theta + \mathbf{u}_{\text{vort}}, \quad x(t) \in \Gamma_f(t), \quad (4.10)$$

where $\mathbf{u}_{\text{vort}} = \nabla \wedge \varphi$ is defined by $\Delta \varphi = T \mathcal{V}$ and

$$\partial_t \mathcal{V} + \nabla \cdot (\mathbf{u}_{\text{therm}} \mathcal{V}) = S_1, \quad x \in \Omega. \quad (4.11)$$

The thermal velocity is $\mathbf{u}_{\text{therm}} = n T^n \nabla T$. The source term is $S_1 = (\mathbf{g} \cdot \mathbf{n}^\perp|_{\Gamma_f}) \delta_{\Gamma_f(t)}$. A rigorous justification in dimension one is in [46, 47]. We quote the works of Gil and Quiros[52] to justify the approximation of (4.8) by (4.9) in dimension strictly greater than one. To our knowledge, the mathematical theory of such models in the context of ICF flows is not understood yet. The first method published for the numerical solution of the Hele-Shaw equation seems to be [68].

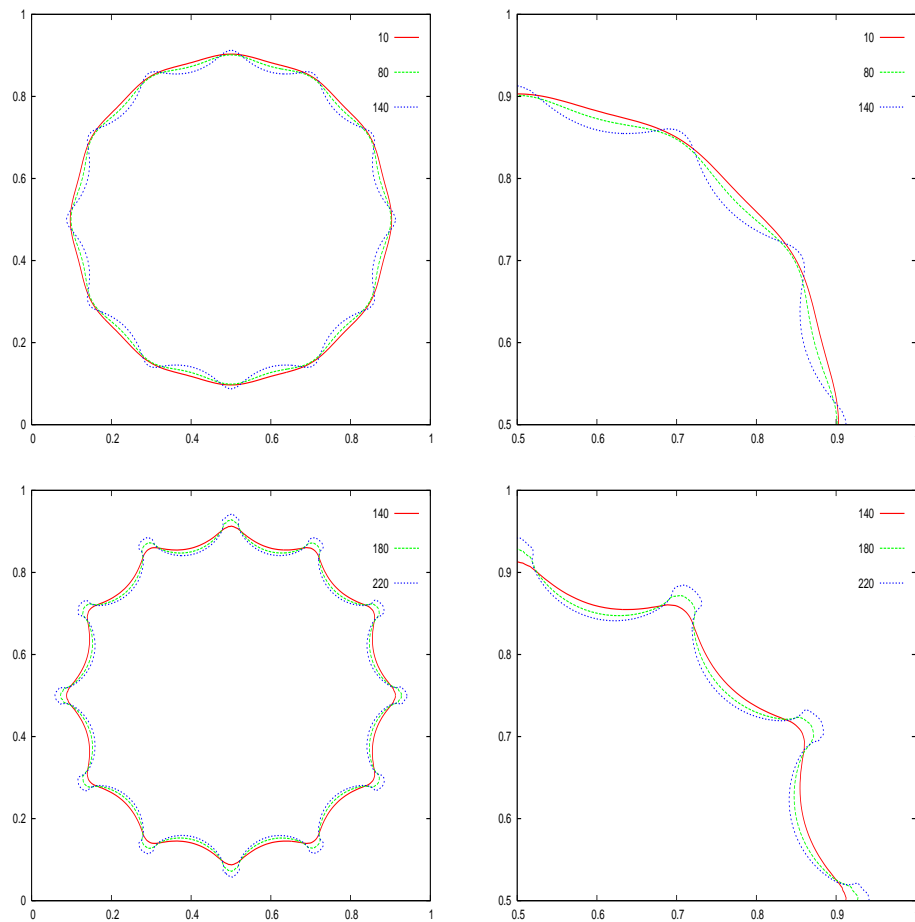


Figure 4.4: This numerical result was obtained by H. Egly [46] using the Fat Boundary Method of Ismail and Maury [102, 71]. The ablation front at five different times (top: $t = 10, 80$ and 140 , bottom: $t = 140, 180$ and 220). The gravity is $g = 1000$. At $t = 0$ the front is discretized with 100 markers with a mode 12. The results show first the development of an instability first in a linear regime, and then in a non linear regime.

Bibliography

- [1] I. Aavatsmark, G.T. Eigestad, R.A. Klausen, M.F. Wheeler, and I. Yotov. Convergence of a symmetric MPFA method on quadrilateral grids. *Comput. Geosci.*, 11(4):333–345, 2007.
- [2] Marvin L. Adams and Paul F. Nowak. Asymptotic analysis of a computational method for time- and frequency-dependent radiative transfer. *Journal of Computational Physics*, 146(1):366 – 403, 1998.
- [3] T. Alazard. Low Mach number limit of the full navier-stokes equations. *Arch. Rat. Mech. Analysis*, 180:1–73, 2006.
- [4] C. Almarcha, P. Clavin, L. Duchemin, and J. Sanz. Ablative Rayleigh-Taylor instability with strong temperature dependence of the thermal conductivity. *J. Fluid. Mech.*, 2007.
- [5] Todd Arbogast, Mary F. Wheeler, and Ivan Yotov. Mixed finite elements for elliptic problems with tensor coefficients as cell-centered finite differences. *SIAM J. Numer. Anal.*, 34(2):828–852, 1997.
- [6] D.G. Aronson. Regularity properties of flows through porous media. *SIAM J. Appl. Math.*, 17:461–467, 1969.
- [7] D.G. Aronson. Regularity properties of flows through porous media: The interface. *Arch. Ration. Mech. Anal.*, 37:1–10, 1970.
- [8] D.G. Aronson, L.A. Caffarelli, and J.L. Vazquez. Interfaces with a corner point in one-dimensional porous medium flow. *Commun. Pure Appl. Math.*, 38:375–404, 1985.
- [9] D. Balsara. Fast and accurate discrete ordinates methods for multidimensional radiative transfer. part i: Basic methods. *J. Quant. Spectro. Radiat. Transfer*, 69:671–707, 2001.
- [10] C. Bardos, F. Golse, and B. Perthame. The radiative transfer equations: Existence of solutions and diffusion approximation under accretivity assumptions - A survey. *Transp. Theory Stat. Phys.*, 16:637–652, 1987.
- [11] C. Bardos, F. Golse, B. Perthame, and R. Sentis. The nonaccretive radiative transfer equations: Existence of solutions and Rosseland approximation. *J. Funct. Anal.*, 77(2):434–460, 1988.
- [12] C. Bardos, R. Santos, and R. Sentis. Diffusion approximation and computation of the critical size. *Trans. Am. Math. Soc.*, 284:617–649, 1984.
- [13] D. J. Benson. Computational methods in Lagrangian and Eulerian hydrocodes. *comp. meth. appl. mech. eng.*, 99:235–394, 1992.
- [14] F. Boyer. Volumes finis pour la résolution de problèmes elliptiques hétérogènes anisotropes sur maillages généraux. <http://www.cmi.univ-mrs.fr/~fboyer/exposes/Roscoff08.pdf>, 2008.
- [15] Jérôme Breil and Pierre-Henri Maire. A cell-centered diffusion scheme on two-dimensional unstructured meshes. *J. Comput. Phys.*, 224(2):785–823, 2007.

- [16] Breil, J. and Hallo, L. and Maire, P.H. and Olazabal-Loumé, M. Hydrodynamic instabilities in axisymmetric geometry. Self-similar models and numerical simulations. *Laser and particle beams*, 23:155–160, 2005.
- [17] Didier Bresch and Benoît Desjardins. On the existence of global weak solutions to the Navier-Stokes equations for viscous compressible and heat conducting fluids. *J. Math. Pures Appl.* (9), 87(1):57–90, 2007.
- [18] Brézis, Haïm and Crandall, Michael G. Uniqueness of solutions of the initial-value problem for $u_t - \Delta\varphi(u) = 0$. *J. Math. Pures et Appl.*, 58:153–163, 1979.
- [19] Franco Brezzi, Annalisa Buffa, and Konstantin Lipnikov. Mimetic finite differences for elliptic problems. *ESAIM, Math. Model. Numer. Anal.*, 43(2):277–295, 2009.
- [20] Franco Brezzi, Konstantin Lipnikov, and Mikhail Shashkov. Convergence of the mimetic finite difference method for diffusion problems on polyhedral meshes. *SIAM J. Numer. Anal.*, 43(5):1872–1896, 2005.
- [21] C. Buet and B. Després. Grey radiative hydrodynamics – hierarchy of models and numerical applications. In C. Berthon, C. Buet, J.-F. Coulombel, B. Després, J. Dubois, T. Goudon, J. E. Morel, and R. Turpault, editors, *Mathematical models and numerical methods for radiative transfer*, volume 28. Société mathématique de France, 2009.
- [22] Christophe Buet and Bruno Després. Asymptotic preserving and positive schemes for radiation hydrodynamics. *J. Comput. Phys.*, 215(2):717–740, 2006.
- [23] D.E Burton. Multidimensionnal discretization of conservation laws for unstructured polyhedral grids. Technical report, Lawrence Livermore National Laboratory, UCRL-JC-118306, 1994.
- [24] E. J. Caramana, D. E. Burton, M. J. Shashkov, and P. P. Whalen. The construction of compatible hydrodynamics algorithms utilizing conservation of total energy. *J. Comput. Phys.*, 146:227–262, 1998.
- [25] E. J. Caramana, M. J. Shashkov, and P. P. Whalen. Formulations of artificial viscosity for multidimensional shock wave computations. *J. Comput. Phys.*, 144:70–97, 1998.
- [26] Carré, G. and Del Pino, S. and Pichon Gostaf, K. and Labourasse, E. and Shapeev, A. V. . Polynomial Least-Squares reconstruction for semi-Lagrangian Cell-Centered Hydrodynamic Schemes. *ESAIM-Proc*, 28:100–116, 2009.
- [27] Castor, J. I. *Radiation Hydrodynamics*. Cambridge University Press, 2004.
- [28] S. Chandrasekhar. *Radiative transfer*. (International Series of Monographs on Physics) Oxford: Clarendon Press; London: Oxford University Press. XIV, 394 p. , 1950.
- [29] Clouët, J-F. and Sentis, R. Milne problem for non-grey radiative transfer. *Kinet. Relat. Models*, 2(2):345–362, 2009.
- [30] Dafermos C.M. *Hyperbolic conservation laws in continuum physics*. Springer Verlag, 2000.
- [31] Collectif DIF. Synthèse des études pour l’allumage thermonucléaire avec 1.8 MJ d’énergie laser (LMJ): théorie et expérience. Technical Report R-6182, CEA/DAM Dif, 2008.
- [32] Yves Coudière, Jean-Paul Vila, and Philippe Villedieu. Convergence rate of a finite volume scheme for a two dimensional convection-diffusion problem. *M2AN, Math. Model. Numer. Anal.*, 33(3):493–516, 1999.
- [33] Jean-François Coulombel, François Golse, and Thierry Goudon. Diffusion approximation and entropy-based moment closure for kinetic equations. *Asymptotic Anal.*, 45(1-2):1–39, 2005.
- [34] Dautray, R. and Watteau, J. P. *La fusion thermonucléaire inertielle par laser, partie 3, volume 2*. Eyrolles, commissariat à l’énergie atomique, 1993.

- [35] S. Delpino, B. Després, E. Labourasse, and G. Carre. A cell-centered Lagrangian hydrodynamics scheme on general unstructured meshes in arbitrary dimension. *J. Comput. Phys.*, 228:5160–5183, 2009.
- [36] B. Després. Weak consistency of the cell-centered glace scheme on general meshes in any dimension. To appear in *Comp. Meth. Appl. Mech. Eng.*
- [37] B. Després. *Lois de conservation eulériennes, lagrangiennes, et méthodes numériques*. SMAI, 2010.
- [38] B. Després and C. Mazeran. Symmetrization of Lagrangian gas dynamics and Lagrangian solvers. *Comptes Rendus Académie des Sciences (Paris)*, 331:475–480, 2003.
- [39] B. Després and C. Mazeran. Lagrangian gas dynamics in 2D and lagrangian systems. *Arch. Rat. Mech. anal.*, 178:327–372, 2005.
- [40] J. Droniou and C. Le Potier. Construction and convergence study of local-maximum principle preserving schemes for elliptic equations. submitted to *SIAM J. Num. Anal.*
- [41] Bruno Dubroca and Jean-Luc Feugeas. Theoretical and numerical study on a moment closure hierarchy for the radiative transfer equation. (Étude théorique et numérique d’une hiérarchie de modèles aux moments pour le transfert radiatif). *C. R. Acad. Sci. Paris, Ser. I*, 1999.
- [42] Bernard Ducomet and Sárka Necasová. Global existence of solutions for the one-dimensional motions of a compressible viscous gas with radiation: An "infrarelativistic model". *Nonlinear Analysis: Theory, Methods & Applications*, 72(7-8):3258 – 3274, 2010.
- [43] J. K. Dukowicz and B. Meltz. Vorticity errors in multidimensional Lagrangian codes. *J. Comput. Phys.*, 99, 1992.
- [44] A. S. Eddington. On the radiative equilibrium of the stars. *Mon. Not. R. Astr. Soc.*, 77:16, 1916.
- [45] P. Edström. A fast and stable solution method for the radiative transfer problem. *SIAM Rev.*, 47:447–468, 2005.
- [46] H. Egly. *Contribution to modelization and simulation of abaltive-like Rayleigh-Taylor instabilities for ICF*. PhD thesis, Université de Paris 6, 2007.
- [47] H. Egly, B. Després, and R. Sentis. An ablative Hele-Shaw model for ICF flows, modeling and numerical simulations. in preparation.
- [48] R. Eymard, T. Gallouët, and R. Herbin. Discretization of heterogeneous and anisotropic diffusion on general nonconforming meshes sushi: a scheme using stabilization and hybrid interfaces. to appear in *IMA J. of Num. Anal.*
- [49] R. Eymard, T. Gallouët, and R. Herbin. Finite volume methods. In Ph. G. Ciarlet and J.-L. Lions, editors, *Handbook of numerical analysis*, volume VII. North-Holland, Amsterdam, 2000.
- [50] D. P. Flanagan and T. Belytshko. A uniform strain hexaedron and quadrilateral and orthogonal hourglass control. *Int. J. Numer. Meth. Engrg.*, 17:679–706, 1982.
- [51] Kluth G. and Després B. Discretization of hyperelasticity on unstructured mesh with a cell centered scheme. Technical Report R09063, LJLL, UPMC, Paris, 2009.
- [52] O. Gil and F. Quiros. Convergence of the porous media equation to Hele-Shaw. *Nonlinear Analysis*, 44:1111–1131, 2001.
- [53] E. Godlewski and P.A. P.A. Raviart. *Numerical approximation of hyperbolic systems of conservation laws*. Springer Verlag New York, AMS 118, 118, 1996.

- [54] S. Godunov. A difference scheme for numerical computation of discontinuous solution of hydrodynamic equations. *Math. Sib.*, 47, 1959.
- [55] S. Godunov. Reminiscences about difference schemes. *J. Comput. Phys.*, 153:6–25, 1999.
- [56] F. Golse and B. Perthame. Generalized solutions of the radiative transfer equations in a singular case. *Comm. Math. Phys.*, 106(2):211–239, 1986.
- [57] François Golse. The Milne problem for the radiative transfer equations (with frequency dependence). *Trans. Am. Math. Soc.*, 303:125–143, 1987.
- [58] François Golse, Shi Jin, and C. David Levermore. The convergence of numerical transfer schemes in diffusive regimes. I: Discrete-ordinate method. *SIAM J. Numer. Anal.*, 36(5):1333–1369, 1999.
- [59] François Golse, Shi Jin, and C. David Levermore. A domain decomposition analysis for a two-scale linear transport problem. *M2AN, Math. Model. Numer. Anal.*, 37(6):869–892, 2003.
- [60] Laurent Gosse and Giuseppe Toscani. Asymptotic-preserving and well-balanced schemes for radiative transfer and the Rosseland approximation. *Numer. Math.*, 98(2):223–250, 2004.
- [61] H. Guillard and A. Murrone. On the behavior of the upwind scheme in low Mach number limit, ii. *Computer Fluids*, 33:655–675, 2004.
- [62] Cory D. Hauck, C. David Levermore, and André L. Tits. Convex duality and entropy-based moment closures: characterizing degenerate densities. *SIAM J. Control Optim.*, 47(4):1977–2015, 2008.
- [63] F. Hermeline. Approximation of diffusion operators with discontinuous tensor coefficients on distorted meshes. *Comput. Methods Appl. Mech. Eng.*, 192(16-18):1939–1959, 2003.
- [64] F. Hermeline. Approximation of 2D and 3D diffusion operators with variable full tensor coefficients on arbitrary meshes. *Comput. Methods Appl. Mech. Eng.*, 196(21-24):2497–2526, 2007.
- [65] F. Hermeline. *Nouvelles méthodes de volumes finis pour approcher des équations aux dérivées partielles sur des maillages quelconques*. Habilitation à diriger des recherches, CEA/DAM Ile de France, 2008.
- [66] F. Hermeline. A finite volume method for approximating 3D diffusion operators on general meshes. *J. Comput. Phys.*, 228(16):5763–5786, 2009.
- [67] François Hermeline. A finite volume method for second-order elliptic equations. (Une méthode de volumes finis pour les équations elliptiques du second ordre.). *C. R. Acad. Sci. Paris, Ser. I*, 1998.
- [68] S. D. Howison and J. M. Aitchison. Numerical computation of Hele-Shaw flows with free boundaries. *J. Comp. Phys.*, 1985.
- [69] W. B. Hubbard. Studies in stellar evolution. v. transport coefficients of degenerate stellar matter. *Astrophys. J.*, 146:858, 1966.
- [70] W. H. Hui. Unified coordinate system in computational fluid dynamics. *Comm. Comp. Phys.*, 2:577–610, 2006.
- [71] M. Ismail and B. Maury. The Fat Boundary Method for the numerical resolution of elliptic problems in perforated domains. Application to 3d fluid flows. *Proc. du 35ème Congrès Nat. d’Ana. Num.*, pages 1–25, 2003.
- [72] Peng Jiang and Dehua Wang. Formation of singularities of solutions to the three-dimensional Euler-Boltzmann equations in radiation hydrodynamics. *Nonlinearity*, 23(4):809–821, 2010.

- [73] Shi Jin and C. David Levermore. Fully-discrete numerical transfer in diffusive regimes. *Transp. Theory Stat. Phys.*, 22(6):739–791, 1993.
- [74] M. Katoh and S. Sakashita. Flux limited diffusion theory in a moving fluid. *Astrophys. Space Sci.*, 203(2):275–288, 1993.
- [75] David S. Kershaw. Differencing of the diffusion equation in Lagrangian hydrodynamic codes. *J. Comput. Phys.*, 39:375–395, 1981.
- [76] Robert Kersner. Degenerate parabolic equations with general nonlinearities. *Nonlinear Anal., Theory Methods Appl.*, 4:1043–1062, 1980.
- [77] R. Kidder. Laser driven compression of hollow shells: power requirements and stability limitations. *Nucl. Fus.*, 1:3–14, 1976.
- [78] Barry F. Knerr. The porous medium equation in one dimension. *Trans. Am. Math. Soc.*, 234:381–415, 1977.
- [79] B. Lapeyre, E. Pardoux, and R. Sentis. *Méthodes de Monte Carlo pour les équations de transport et de diffusion*. Number 29 in Mathématiques & Applications. Springer-Verlag, 1998.
- [80] E. W. Larsen, G. C. Pomraning, and V. C. Badham. Asymptotic analysis of radiative transfer problems. *Journal of Quantitative Spectroscopy and Radiative Transfer*, 29:285–310, April 1983.
- [81] Edward W. Larsen, Guido Thömmes, and Axel Klar. New frequency-averaged approximations to the equations of radiative heat transfer. *SIAM J. Appl. Math.*, 64(2):565–582 (electronic), 2003/04.
- [82] Edward W. Larsen, Guido Thömmes, Axel Klar, Mohammed Seaïd, and Thomas Götz. Simplified P_N approximations to the equations of radiative heat transfer and applications. *J. Comput. Phys.*, 183(2):652–675, 2002.
- [83] Sébastien Lasserre. *Contribution à l'étude mathématique et numérique des solutions à support compact pour les modèles de turbulence compressible*. PhD thesis, Université de Paris 6, 2005.
- [84] J. D. Lawson. Some criteria for a power producing thermonuclear reactor. *Proc. Phys. Soc. B*, 70(1):6–11, 1957.
- [85] Christophe Le Potier. A linear scheme satisfying a maximum principle for anisotropic diffusion operators on distorted grids. (Un schéma linéaire vérifiant le principe du maximum pour des opérateurs de diffusion très anisotropes sur des maillages déformés.). *C. R., Math., Acad. Sci. Paris*, 347(1-2):105–110, 2009.
- [86] J. R. Leveque. Numerical methods for conservation laws. *Lectures in Mathematics*, 1991. Birkhauser.
- [87] C. D. Levermore. Relating eddington factors to flux limiters. *Journal of Quantitative Spectroscopy and Radiative Transfer*, 31(2):149 – 160, 1984.
- [88] C. D. Levermore and G. C. Pomraning. A flux-limited diffusion theory. *Astrophys. J.*, 248:321–334, 1981.
- [89] C. David Levermore. Entropy-based moment closures for kinetic equations. *Transp. Theory Stat. Phys.*, 26(4-5):591–606, 1997.
- [90] E. E. Lewis and J. W. F. Miller. *Computational methods of neutron transport*. American Nuclear Society, La Grange Park, Illinois, 1993.

- [91] C. Lin. *Modèles mathématiques de la théorie du transfert radiatif [mathematical models for the radiative transfer theory]*. PhD thesis, Université des Sciences et Technologie de Lille - Lille I, 2007.
- [92] J. D. Lindl. *Inertial Confinement Fusion*, 1998.
- [93] Konstantin Lipnikov, Mikhail Shashkov, and Ivan Yotov. Local flux mimetic finite difference methods. *Numer. Math.*, 112(1):115–152, 2009.
- [94] Óscar López-Pouso. Trace theorem and existence in radiation. *Adv. Math. Sci. Appl.*, 10(2):757–773, 2000.
- [95] J. F. Luciani, P. Mora, and R. Pellat. Quasistatic heat front and delocalized heat flux. *Physics of Fluids*, 28(3):835–845, 1985.
- [96] J. F. Luciani, P. Mora, and J. Virmont. Nonlocal heat transport due to steep temperature gradients. *Phys. Rev. Lett.*, 51(18):1664–1667, Oct 1983.
- [97] P. H. Maire, R. Abgrall, J. Breil, and J. Ovadia. A cell-centered lagrangian scheme for 2D compressible flow problems. *Siam J. Sci. Comp.*, 29, 2007.
- [98] P.H. Maire. A high-order cell centered lagrangian scheme for two-dimensional compressible fluid flows on unstructured meshes. *J. Comput. Phys.*, online, 2009.
- [99] P.H. Maire and B. Nkonga. Multi-scale Godunov type method for cell-centered discrete lagrangian hydrodynamics. *J. Comput. Phys.*, 2009.
- [100] R. E. Marshak. Effect of radiation on shock wave behavior. *Phys. Fluids*, 1:24, 1958.
- [101] L. Masse. *Etude linéaire de l'instabilité du front d'ablation en fusion par confinement inertiel*. PhD thesis, Université d'Aix-Marseille, 2001.
- [102] B. Maury. A Fat Boundary Method for the Poisson equation in a domain with holes. *J. of Sci. Computing*, 16(3):319–339, 2001.
- [103] B. Mercier. Application of accretive operators theory to the radiative transfer equations. *SIAM J. Math. Anal.*, 18(2):393–408, 1987.
- [104] Dimitri Mihalas and Barbara Weibel Mihalas. *Foundations of radiation hydrodynamics*. New York etc.: Oxford University Press. XV, 718 p.; \$ 75.00 , 1984.
- [105] Gerald N. Minerbo. Maximum entropy eddington factors. *Journal of Quantitative Spectroscopy and Radiative Transfer*, 20(6):541 – 545, 1978.
- [106] I. D. Mishev. Finite volume methods on voronoi meshes. *Numer. Meth. P.D.E.*, 14:193–212, 1998.
- [107] J. E. Morel. Diffusion-limit asymptotics of the transport equation, the p1/3 equations, and two flux-limited diffusion theories. *Journal of Quantitative Spectroscopy and Radiative Transfer*, 65(5):769 – 778, 2000.
- [108] J. E. Morel. Discrete-ordinates transport methods for non-relativistic radiation-hydrodynamics. In C. Berthon, C. Buet, J.-F. Coulombel, B. Després, J. Dubois, T. Goudon, J. E. Morel, and R. Turpault, editors, *Mathematical models and numerical methods for radiative transfer*, volume 28. Société mathématique de France, 2009.
- [109] J. von Neumann and R. D. Richtmyer. A method for the calculation of hydrodynamics shocks. *J. appl. Phys.*, 21:232–237, 1950.
- [110] R.E. Pattle. Diffusion from an instantaneous point source with a concentration- dependent coefficient. *Q. J. Mech. Appl. Math.*, 12:407–409, 1959.

- [111] Sanz J. Piriz A.R. and Ibanez L.F. Rayleigh-Taylor Instability of steady ablation front: The discontinuity model revised. *Phys. Plasmas*, 4(4), 1997.
- [112] G. C. Pomraning. *The equation of radiation hydrodynamics*. Pergamon Press, 1973.
- [113] G. C. Pomraning. The non-equilibrium marshak wave problem. *Journal of Quantitative Spectroscopy and Radiative Transfer*, 21(3):249 – 261, 1979.
- [114] G. C. Pomraning. Flux-limited diffusion with relativistic corrections. *Astrophys. J.*, 266:841–847, 1983.
- [115] Maria Michaela Porzio and Óscar López-Pouso. Application of accretive operators theory to evolutive combined conduction, convection and radiation. *Rev. Mat. Iberoamericana*, 20(1):257–275, 2004.
- [116] W. E. Pracht. Calculating three-dimensional fluid flows at all speeds with an Eulerian-Lagrangian computing mesh. *J. Comput. Phys.*, 17:132–159, 1975.
- [117] S. Rosseland. The principles of quantum theory. *Handb. der Astrophys.*, 3(1):443, 1930.
- [118] Saillard, Y. Hydrodynamique de l’implosion d’une cible FCI . *CRAS*, t 1, série IV:705–718, 2000.
- [119] J. Sanz. Self-consistent analytical model of the Rayleigh-Taylor instability in inertial confinement fusion. *Phys. Rev. Lett.*, 73:2700–2703, 1994.
- [120] J. Sanz and al. Nonlinear Theory of the Ablative Rayleigh-Taylor Instability. *Phys. Review Letter*, 89(19), 2002.
- [121] B Scheurer. Quelques schémas numériques pour l’hydrodynamique lagrangienne. Technical report, Commissariat à l’Energie Atomique, CEA-R-5942, 2000.
- [122] G. P. Schurtz, Ph. D. Nicolai, and M. Busquet. A nonlocal electron conduction model for multidimensional radiation hydrodynamics codes. *Physics of Plasmas*, 7(10):4238–4249, 2000.
- [123] G. Scovazzi. A discourse on Galilean invariance, SUPG stabilization, and the variational multiscale framework. *Comp. Method. Appl. Mech. Eng.*, 54(6-8):1108–1132, 2007.
- [124] G. Scovazzi. Galilean invariance and stabilized methods for compressible flows. *Int. J. Num. Meth. Fluids*, 54(6-8):757–778, 2007.
- [125] G. Scovazzi. Stabilized shock hydrodynamics: II. Design and physical interpretation of the SUPG operator for Lagrangian computations. *Comp. Method. Appl. Mech. Eng.*, 196(4-6):967–978, 2007.
- [126] G. Scovazzi, M. A; Christon, T. J. R. Hugues, and J. N. Shadid. Stabilized shock hydrodynamics: I. A Lagrangian method. *Comp. Method. Appl. Mech. Eng.*, 196(4-6):923–966, 2007.
- [127] G. Scovazzi, E. Love, and M.J. Shashkov. Multi-scale Lagrangian shock hydrodynamics on Q1/P0 finite elements: Theoretical framework and two-dimensional computations. *Comp. Meth. in Applied Mech. and Eng.*, 197:1056–1079, 2008.
- [128] R. Sentis. Half space problems for frequency dependent transport equations. Application to the Rosseland approximation of the radiative transfer equations. *Transp. Theory Stat. Phys.*, 16:653–697, 1987.
- [129] Sentis, R. *Mathematical Models and Methods for Plasma Physics*. in preparation, 2010.
- [130] D. Serre. *Systèmes de lois de conservation*. Diderot, 1996.
- [131] M. Shashkov. *Conservative finite difference methods on general grids*. CRC Press, 1996.

- [132] Shkarofsky, I. P. and Johnston, T. W. and Bachynski, M. P. *The particle kinetics of plasmas*. Addison Wesley Publishing Company, 1966.
- [133] V. Siess. in preparation.
- [134] V. Siess. A linear and accurate diffusion scheme respecting the maximum principle on distorted meshes. *C. R. Acad. Sci. Paris, Ser. I*, 347:1317–1320, 2009.
- [135] Lyman Spitzer and Richard Härm. Transport phenomena in a completely ionized gas. *Phys. Rev.*, 89(5):977–981, Mar 1953.
- [136] Bingjing Su and Gordon L. Olson. An analytical benchmark for non-equilibrium radiative transfer in an isotropically scattering medium. *Annals of Nuclear Energy*, 24(13):1035 – 1055, 1997.
- [137] N. Sukumar. Voronoi cell finite difference method for the diffusion operator on arbitrary unstructured grids. *Int. J. Numer. Meth. Engng.*, 57:1–34, 2003.
- [138] Monthieth L. Takabe H., Mima K. and Morse R. Self-consistent of the Rayleigh-Taylor instability in ablatively accelerated plasma. *Phys. Fluids*, 28:3676–3682, 1985.
- [139] E. Toro. *Riemann solvers and numerical methods for fluid dynamics. Second edition*. Springer-Verlag, 1999.
- [140] N. J. Turner and J. M. Stone. A module for radiation hydrodynamic calculations with zeus-2d using flux-limited diffusion. *Astrophys. J. Suppl. Ser.*, 135:95–107, 2001.
- [141] Rodolphe Turpault. A consistent multigroup model for radiative transfer and its underlying mean opacities. *Journal of Quantitative Spectroscopy and Radiative Transfer*, 94(3-4):357 – 371, 2005.
- [142] Juan L. Vazquez. Behaviour of the velocity of one-dimensional flows in porous media. *Trans. Am. Math. Soc.*, 286:787–802, 1984.
- [143] M. Vohralik and B. Wohlmuth. Mixed finite element methods: implementation with one unknown per element, local flux expressions, positivity, polygonal meshes, and relations to other methods. to appear.
- [144] D. Wagner. Equivalence of the eulerian and lagrangian equations of gas dynamics for weak solutions. *Journal of Differential Equations*, 68:118–136, 1987.
- [145] M. Wilkins. Use of artificial viscosity in multidimensional shock wave problems. *J. Comput. Phys.*, 3(36):281–303, 1980.
- [146] Zel’dovich, Ya. B. and Raiser, Yu. *Physics of Shock Waves and High Temperature Hydrodynamic Phenomena*. Academic Press, New York, 1966.
- [147] Xinhua Zhong and Song Jiang. Local existence and finite-time blow-up in multidimensional radiation hydrodynamics. *J. Math. Fluid Mech.*, 9(4):543–564, 2007.